5.16 Plane A flying at a speed of 900 km/hr with respect to the ground is approaching plane B. Plane A's Doppler radar, operating at the X-band frequency of 10 GHz, detects a positive Doppler shift of 2 kHz in the return frequency. Determine the speed of plane B with respect to the ground. [*Ans.* 792 km/hr.]

5.17 The complete set of Lorentz transformations of the fields in Eq. (5.8.8) is as follows (see also Eq. (K.31) of Appendix K):

$$E_x = \gamma(E'_x + \beta c B'_y), \quad H_y = \gamma(H'_y + c\beta D'_x), \quad D_x = \gamma(D'_x + \frac{1}{c}\beta H'_y), \quad B_y = \gamma(B'_y + \frac{1}{c}\beta E'_x)$$

The constitutive relations in the rest frame S' of the moving dielectric are the usual ones, that is, $B'_y = \mu H'_y$ and $D'_x = \epsilon E'_x$. By eliminating the primed quantities in terms of the unprimed ones, show that the constitutive relations have the following form in the fixed system S:

$$D_x = \frac{(1-\beta^2)\epsilon E_x - \beta(n^2-1)H_y/c}{1-\beta^2 n^2}, \quad B_y = \frac{(1-\beta^2)\mu H_y - \beta(n^2-1)E_x/c}{1-\beta^2 n^2}$$

where n is the refractive index of the moving medium, $n = \sqrt{\epsilon\mu/\epsilon_0\mu_0}$. Show that for free space, the constitutive relations remain the same as in the frame S'.

6

Multilayer Structures

Higher-order transfer functions of the type of Eq. (5.7.2) can achieve broader reflectionless notches and are used in the design of thin-film antireflection coatings, dielectric mirrors, and optical interference filters [632–694,754–787], and in the design of broadband terminations of transmission lines [822–832].

They are also used in the analysis, synthesis, and simulation of fiber Bragg gratings [788–808], in the design of narrow-band transmission filters for wavelength-division multiplexing (WDM), and in other fiber-optic signal processing systems [818–821].

They are used routinely in making acoustic tube models for the analysis and synthesis of speech, with the layer recursions being mathematically equivalent to the Levinson lattice recursions of linear prediction [833–839]. The layer recursions are also used in speech recognition, disguised as the Schur algorithm.

They also find application in geophysical deconvolution and inverse scattering problems for oil exploration [840–849].

The layer recursions—known as the Schur recursions in this context—are intimately connected to the mathematical theory of lossless bounded real functions in the z-plane and positive real functions in the s-plane and find application in network analysis, synthesis, and stability [853–867].

6.1 Multiple Dielectric Slabs

The general case of arbitrary number of dielectric slabs of arbitrary thicknesses is shown in Fig. 6.1.1. There are M slabs, $M+1$ interfaces, and $M+2$ dielectric media, including the left and right semi-infinite media η_a and η_b.

The incident and reflected fields are considered at the *left* of each interface. The overall reflection response, $\Gamma_1 = E_{1-}/E_{1+}$, can be obtained recursively in a variety of ways, such as by the propagation matrices, the propagation of the impedances at the interfaces, or the propagation of the reflection responses.

The elementary reflection coefficients ρ_i from the left of each interface are defined in terms of the characteristic impedances or refractive indices as follows:

$$\rho_i = \frac{\eta_i - \eta_{i-1}}{\eta_i + \eta_{i-1}} = \frac{n_{i-1} - n_i}{n_{i-1} + n_i}, \quad i = 1, 2, \ldots, M+1 \tag{6.1.1}$$

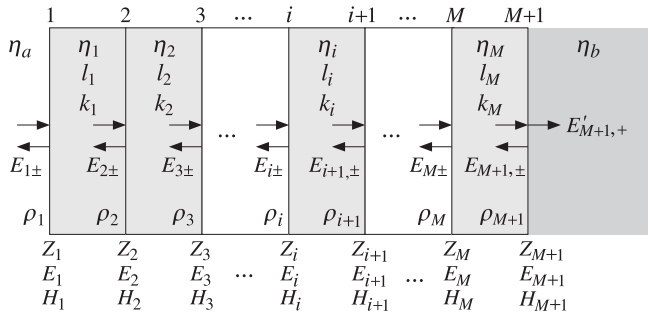

Fig. 6.1.1 Multilayer dielectric slab structure.

where $\eta_i = \eta_0/n_i$, and we must use the convention $n_0 = n_a$ and $n_{M+1} = n_b$, so that $\rho_1 = (n_a - n_1)/(n_a + n_1)$ and $\rho_{M+1} = (n_M - n_b)/(n_M + n_b)$. The forward/backward fields at the left of interface i are related to those at the left of interface $i+1$ by:

$$\begin{bmatrix} E_{i+} \\ E_{i-} \end{bmatrix} = \frac{1}{\tau_i} \begin{bmatrix} e^{jk_il_i} & \rho_i e^{-jk_il_i} \\ \rho_i e^{jk_il_i} & e^{-jk_il_i} \end{bmatrix} \begin{bmatrix} E_{i+1,+} \\ E_{i+1,-} \end{bmatrix}, \quad i = M, M-1, \ldots, 1 \tag{6.1.2}$$

where $\tau_i = 1 + \rho_i$ and k_il_i is the phase thickness of the ith slab, which can be expressed in terms of its optical thickness n_il_i and the operating free-space wavelength by $k_il_i = 2\pi(n_il_i)/\lambda$. Assuming no backward waves in the right-most medium, these recursions are initialized at the $(M+1)$st interface as follows:

$$\begin{bmatrix} E_{M+1,+} \\ E_{M+1,-} \end{bmatrix} = \frac{1}{\tau_{M+1}} \begin{bmatrix} 1 & \rho_{M+1} \\ \rho_{M+1} & 1 \end{bmatrix} \begin{bmatrix} E'_{M+1,+} \\ 0 \end{bmatrix} = \frac{1}{\tau_{M+1}} \begin{bmatrix} 1 \\ \rho_{M+1} \end{bmatrix} E'_{M+1,+}$$

It follows that the reflection responses $\Gamma_i = E_{i-}/E_{i+}$ will satisfy the recursions:

$$\boxed{\Gamma_i = \frac{\rho_i + \Gamma_{i+1}e^{-2jk_il_i}}{1 + \rho_i\Gamma_{i+1}e^{-2jk_il_i}}}, \qquad i = M, M-1, \ldots, 1 \tag{6.1.3}$$

and initialized by $\Gamma_{M+1} = \rho_{M+1}$. Similarly the recursions for the total electric and magnetic fields, which are continuous across each interface, are given by:

$$\begin{bmatrix} E_i \\ H_i \end{bmatrix} = \begin{bmatrix} \cos k_il_i & j\eta_i \sin k_il_i \\ j\eta_i^{-1} \sin k_il_i & \cos k_il_i \end{bmatrix} \begin{bmatrix} E_{i+1} \\ H_{i+1} \end{bmatrix}, \quad i = M, M-1, \ldots, 1 \tag{6.1.4}$$

and initialized at the $(M+1)$st interface as follows:

$$\begin{bmatrix} E_{M+1} \\ H_{M+1} \end{bmatrix} = \begin{bmatrix} 1 \\ \eta_b^{-1} \end{bmatrix} E'_{M+1,+}$$

It follows that the impedances at the interfaces, $Z_i = E_i/H_i$, satisfy the recursions:

$$\boxed{Z_i = \eta_i \frac{Z_{i+1} + j\eta_i \tan k_il_i}{\eta_i + jZ_{i+1} \tan k_il_i}}, \quad i = M, M-1, \ldots, 1 \tag{6.1.5}$$

and initialized by $Z_{M+1} = \eta_b$. The objective of all these recursions is to obtain the overall reflection response Γ_1 into medium η_a.

The MATLAB function `multidiel` implements the recursions (6.1.3) for such a *multi-dielectric* structure and evaluates Γ_1 and Z_1 at any desired set of free-space wavelengths. Its usage is as follows:

```
[Gamma1,Z1] = multidiel(n,L,lambda);          % multilayer dielectric structure
```

where n, L are the vectors of refractive indices of the $M+2$ media and the optical thicknesses of the M slabs, that is, in the notation of Fig. 6.1.1:

$$n = [n_a, n_1, n_2, \ldots, n_M, n_b], \quad L = [n_1l_1, n_2l_2, \ldots, n_Ml_M]$$

and λ is a vector of free-space wavelengths at which to evaluate Γ_1. Both the optical lengths L and the wavelengths λ are in units of some desired reference wavelength, say λ_0, typically chosen at the center of the desired band. The usage of `multidiel` was illustrated in Example 5.5.2. Additional examples are given in the next sections.

The layer recursions (6.1.2)–(6.1.5) remain essentially unchanged in the case of oblique incidence (with appropriate redefinitions of the impedances η_i) and are discussed in Chap. 7.

Next, we apply the layer recursions to the analysis and design of antireflection coatings and dielectric mirrors.

6.2 Antireflection Coatings

The simplest example of antireflection coating is the quarter-wavelength layer discussed in Example 5.5.2. Its primary drawback is that it requires the layer's refractive index to satisfy the reflectionless condition $n_1 = \sqrt{n_an_b}$.

For a typical glass substrate with index $n_b = 1.50$, we have $n_1 = 1.22$. Materials with n_1 near this value, such as magnesium fluoride with $n_1 = 1.38$, will result into some, but minimized, reflection compared to the uncoated glass case, as we saw in Example 5.5.2.

The use of multiple layers can improve the reflectionless properties of the single quarter-wavelength layer, while allowing the use of real materials. In this section, we consider three such examples.

Assuming a magnesium fluoride film and adding between it and the glass another film of higher refractive index, it is possible to achieve a reflectionless structure (at a single wavelength) by properly adjusting the film thicknesses [634,659].

With reference to the notation of Fig. 5.7.1, we have $n_a = 1$, $n_1 = 1.38$, n_2 to be determined, and $n_b = n_{\text{glass}} = 1.5$. The reflection response at interface-1 is related to the response at interface-2 by the layer recursions:

$$\Gamma_1 = \frac{\rho_1 + \Gamma_2e^{-2jk_1l_1}}{1 + \rho_1\Gamma_2e^{-2jk_1l_1}}, \quad \Gamma_2 = \frac{\rho_2 + \rho_3e^{-2jk_2l_2}}{1 + \rho_2\rho_3e^{-2jk_2l_2}}$$

The reflectionless condition is $\Gamma_1 = 0$ at an operating free-space wavelength λ_0. This requires that $\rho_1 + \Gamma_2 e^{-2jk_1l_1} = 0$, which can be written as:

$$e^{2jk_1l_1} = -\frac{\Gamma_2}{\rho_1} \tag{6.2.1}$$

Because the left-hand side has unit magnitude, we must have the condition $|\Gamma_2| = |\rho_1|$, or, $|\Gamma_2|^2 = \rho_1^2$, which is written as:

$$\left| \frac{\rho_2 + \rho_3 e^{-2jk_2l_2}}{1 + \rho_2\rho_3 e^{-2jk_2l_2}} \right|^2 = \frac{\rho_2^2 + \rho_3^2 + 2\rho_2\rho_3 \cos 2k_2l_2}{1 + \rho_2^2\rho_3^2 + 2\rho_2\rho_3 \cos 2k_2l_2} = \rho_1^2$$

This can be solved for $\cos 2k_2l_2$:

$$\cos 2k_2l_2 = \frac{\rho_1^2(1 + \rho_2^2\rho_3^2) - (\rho_2^2 + \rho_3^2)}{2\rho_2\rho_3(1 - \rho_1^2)}$$

Using the identity, $\cos 2k_2l_2 = 2\cos^2 k_2l_2 - 1$, we also find:

$$\begin{aligned} \cos^2 k_2l_2 &= \frac{\rho_1^2(1 - \rho_2\rho_3)^2 - (\rho_2 - \rho_3)^2}{4\rho_2\rho_3(1 - \rho_1^2)} \\ \sin^2 k_2l_2 &= \frac{(\rho_2 + \rho_3)^2 - \rho_1^2(1 + \rho_2\rho_3)^2}{4\rho_2\rho_3(1 - \rho_1^2)} \end{aligned} \tag{6.2.2}$$

It is evident from these expressions that not every combination of ρ_1, ρ_2, ρ_3 will admit a solution because the left-hand sides are positive and less than one. If we assume that $n_2 > n_1$ and $n_2 > n_b$, then, we will have $\rho_2 < 0$ and $\rho_3 > 0$. Then, it is necessary that the numerators of above expressions be negative, resulting into the conditions:

$$\left| \frac{\rho_3 + \rho_2}{1 + \rho_2\rho_3} \right|^2 < \rho_1^2 < \left| \frac{\rho_3 - \rho_2}{1 - \rho_2\rho_3} \right|^2$$

The left inequality requires that $\sqrt{n_b} < n_1 < n_b$, which is satisfied with the choices $n_1 = 1.38$ and $n_b = 1.5$. Similarly, the right inequality is violated—and therefore there is no solution—if $\sqrt{n_b} < n_2 < n_1\sqrt{n_b}$, which has the numerical range $1.22 < n_2 < 1.69$.

Catalan [634,659] used bismuth oxide (Bi_2O_3) with $n_2 = 2.45$, which satisfies the above conditions for the existence of solution. With this choice, the reflection coefficients are $\rho_1 = -0.16$, $\rho_2 = -0.28$, and $\rho_3 = 0.24$. Solving Eq. (6.2.2) for k_2l_2 and then Eq. (6.2.1) for k_1l_1, we find:

$$k_1l_1 = 2.0696, \quad k_2l_2 = 0.2848 \quad \text{(radians)}$$

Writing $k_1l_1 = 2\pi(n_1l_1)/\lambda_0$, we find the optical lengths:

$$n_1l_1 = 0.3294\lambda_0, \quad n_2l_2 = 0.0453\lambda_0$$

Fig. 6.2.1 shows the resulting reflection response Γ_1 as a function of the free-space wavelength λ, with λ_0 chosen to correspond to the middle of the visible spectrum, $\lambda_0 = 550$ nm. The figure also shows the responses of the single quarter-wave slab of Example 5.5.2.

The reflection responses were computed with the help of the MATLAB function `multidiel`. The MATLAB code used to implement this example was as follows:

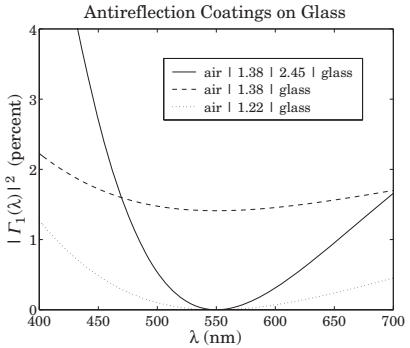

Fig. 6.2.1 Two-slab reflectionless coating.

```
na=1; nb=1.5; n1=1.38; n2=2.45;
n = [na,n1,n2,nb]; la0 = 550;
r = n2r(n);

c = sqrt((r(1)^2*(1-r(2)*r(3))^2 - (r(2)-r(3))^2)/(4*r(2)*r(3)*(1-r(1)^2)));
k2l2 = acos(c);
G2 = (r(2)+r(3)*exp(-2*j*k2l2))/(1 + r(2)*r(3)*exp(-2*j*k2l2));
k1l1 = (angle(G2) - pi - angle(r(1)))/2;
if k1l1 <0, k1l1 = k1l1 + 2*pi; end

L = [k1l1,k2l2]/2/pi;

la = linspace(400,700,101);
Ga = abs(multidiel(n, L, la/la0)).^2 * 100;
Gb = abs(multidiel([na,n1,nb], 0.25, la/la0)).^2 * 100;
Gc = abs(multidiel([na,sqrt(nb),nb], 0.25, la/la0)).^2 * 100;

plot(la, Ga, la, Gb, la, Gc);
```

The dependence on λ comes through the quantities k_1l_1 and k_2l_2, for example:

$$k_1l_1 = 2\pi\frac{n_1l_1}{\lambda} = 2\pi\frac{0.3294\lambda_0}{\lambda}$$

Essentially the same method is used in Sec. 13.7 to design 2-section series impedance transformers. The MATLAB function `twosect` of that section implements the design. It can be used to obtain the optical lengths of the layers, and in fact, it produces two possible solutions:

$$L_{12} = \text{twosect}(1,\ 1/1.38,\ 1/2.45,\ 1/1.5) = \begin{bmatrix} 0.3294 & 0.0453 \\ 0.1706 & 0.4547 \end{bmatrix}$$

where each row represents a solution, so that $L_1 = n_1l_1/\lambda_0 = 0.1706$ and $L_2 = n_2l_2/\lambda_0 = 0.4547$ is the second solution. The arguments of `twosect` are the inverses of the refractive indices, which are proportional to the characteristic impedances of the four media.

Although this design method meets its design objectives, it results in a narrower bandwidth compared to that of the ideal single-slab case. Varying n_2 has only a minor effect on the shape of the curve. To widen the bandwidth, and at the same time keep the reflection response low, more than two layers must be used.

A simple approach is to fix the optical thicknesses of the films to some prescribed values, such as quarter-wavelengths, and adjust the refractive indices hoping that the required index values come close to realizable ones [634,660]. Fig. 6.2.2 shows the two possible structures: the quarter-quarter two-film case and the quarter-half-quarter three-film case.

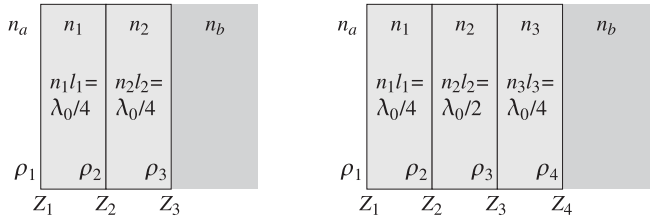

Fig. 6.2.2 Quarter-quarter and quarter-half-quarter antireflection coatings.

The behavior of the two structures is similar at the design wavelength. For the quarter-quarter case, the requirement $Z_1 = \eta_a$ implies:

$$Z_1 = \frac{\eta_1^2}{Z_2} = \frac{\eta_1^2}{\eta_2^2/Z_3} = \frac{\eta_1^2}{\eta_2^2}\eta_b = \eta_a$$

which gives the design condition (see also Example 5.7.1):

$$n_a = \frac{n_1^2}{n_2^2}\, n_b \tag{6.2.3}$$

The optical thicknesses are $n_1 l_1 = n_2 l_2 = \lambda_0/4$. In the quarter-half-quarter case, the half-wavelength layer acts as an absentee layer, that is, $Z_2 = Z_3$, and the resulting design condition is the same:

$$Z_1 = \frac{\eta_1^2}{Z_2} = \frac{\eta_1^2}{Z_3} = \frac{\eta_1^2}{\eta_3^2/Z_4} = \frac{\eta_1^2}{\eta_3^2}\eta_b = \eta_a$$

yielding in the condition:

$$n_a = \frac{n_1^2}{n_3^2}\, n_b \tag{6.2.4}$$

The optical thicknesses are now $n_1 l_1 = n_3 l_3 = \lambda_0/4$ and $n_2 l_2 = \lambda_0/2$. Conditions (6.2.3) and (6.2.4) are the same as far as determining the refractive index of the second quarter-wavelength layer. In the quarter-half-quarter case, the index n_2 of the half-wavelength film is arbitrary.

In the quarter-quarter case, if the first quarter-wave film is magnesium fluoride with $n_1 = 1.38$ and the glass substrate has $n_{\text{glass}} = 1.5$, condition (6.2.3) gives for the index for the second quarter-wave layer:

$$n_2 = \sqrt{\frac{n_1^2 n_b}{n_a}} = \sqrt{\frac{1.38^2 \times 1.50}{1.0}} = 1.69 \tag{6.2.5}$$

The material cerium fluoride (CeF_3) has an index of $n_2 = 1.63$ at $\lambda_0 = 550$ nm and can be used as an approximation to the ideal value of Eq. (6.2.5). Fig. 6.2.3 shows the reflectances $|\Gamma_1|^2$ for the two- and three-layer cases and for the ideal and approximate values of the index of the second quarter-wave layer.

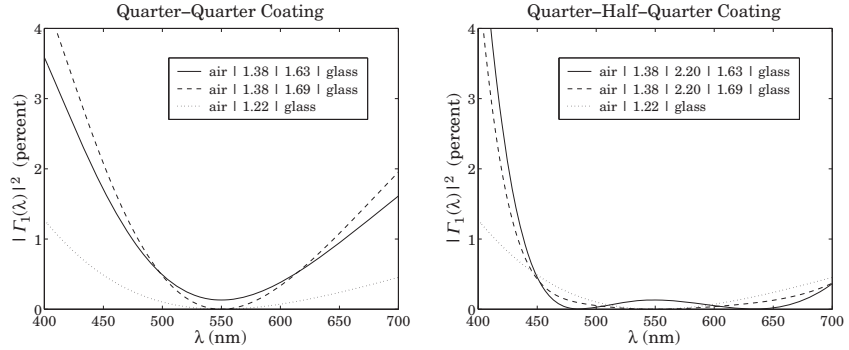

Fig. 6.2.3 Reflectances of the quarter-quarter and quarter-half-quarter cases.

The design wavelength was $\lambda_0 = 550$ nm and the index of the half-wave slab was $n_2 = 2.2$ corresponding to zirconium oxide (ZrO_2). We note that the quarter-half-quarter case achieves a much broader bandwidth over most of the visible spectrum, for either value of the refractive index of the second quarter slab.

The reflectances were computed with the help of the function `multidiel`. The typical MATLAB code was as follows:

```
la0 = 550; la = linspace(400,700,101);

Ga = 100*abs(multidiel([1,1.38,2.2,1.63,1.5], [0.25,0.5,0.25], la/la0)).^2;
Gb = 100*abs(multidiel([1,1.38,2.2,1.69,1.5], [0.25,0.5,0.25], la/la0)).^2;
Gc = 100*abs(multidiel([1,1.22,1.5], 0.25, la/la0)).^2;

plot(la, Ga, la, Gb, la, Gc);
```

These and other methods of designing and manufacturing antireflection coatings for glasses and other substrates can be found in the vast thin-film literature. An incomplete set of references is [632–692]. Some typical materials used in thin-film coatings are given below:

material	n	material	n
cryolite (Na_3AlF_6)	1.35	magnesium fluoride (MgF_2)	1.38
Silicon dioxide SiO_2	1.46	polystyrene	1.60
cerium fluoride (CeF_3)	1.63	lead fluoride (PbF_2)	1.73
Silicon monoxide SiO	1.95	zirconium oxide (ZrO_2)	2.20
zinc sulfide (ZnS)	2.32	titanium dioxide (TiO_2)	2.40
bismuth oxide (Bi_2O_3)	2.45	silicon (Si)	3.50
germanium (Ge)	4.20	tellurium (Te)	4.60

Thin-film coatings have a wide range of applications, such as displays; camera lenses, mirrors, and filters; eyeglasses; coatings for energy-saving lamps and architectural windows; lighting for dental, surgical, and stage environments; heat reflectors for movie projectors; instrumentation, such as interference filters for spectroscopy, beam splitters and mirrors, laser windows, and polarizers; optics of photocopiers and compact disks; optical communications; home appliances, such as heat reflecting oven windows; rear-view mirrors for automobiles.

6.3 Dielectric Mirrors

The main interest in dielectric mirrors is that they have extremely low losses at optical and infrared frequencies, as compared to ordinary metallic mirrors. On the other hand, metallic mirrors reflect over a wider bandwidth than dielectric ones and from all incident angles. However, *omnidirectional dielectric mirrors* are also possible and have recently been constructed [777,778]. The omnidirectional property is discussed in Sec. 8.8. Here, we consider only the normal-incidence case.

A dielectric mirror (also known as a Bragg reflector) consists of identical alternating layers of high and low refractive indices, as shown in Fig. 6.3.1. The optical thicknesses are typically chosen to be quarter-wavelength long, that is, $n_H l_H = n_L l_L = \lambda_0/4$ at some operating wavelength λ_0. The standard arrangement is to have an odd number of layers, with the high index layer being the first and last layer.

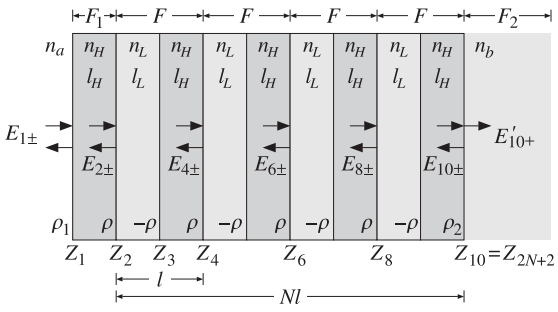

Fig. 6.3.1 Nine-layer dielectric mirror.

Fig. 6.3.1 shows the case of nine layers. If the number of layers is $M = 2N + 1$, the number of interfaces will be $2N + 2$ and the number of media $2N + 3$. After the first

layer, we may view the structure as the repetition of N identical bilayers of low and high index. The elementary reflection coefficients alternate in sign as shown in Fig. 6.3.1 and are given by

$$\rho = \frac{n_H - n_L}{n_H + n_L}, \quad -\rho = \frac{n_L - n_H}{n_L + n_H}, \quad \rho_1 = \frac{n_a - n_H}{n_a + n_H}, \quad \rho_2 = \frac{n_H - n_b}{n_H + n_b} \tag{6.3.1}$$

The substrate n_b can be arbitrary, even the same as the incident medium n_a. In that case, $\rho_2 = -\rho_1$. The reflectivity properties of the structure can be understood by propagating the impedances from bilayer to bilayer. For the example of Fig. 6.3.1, we have for the quarter-wavelength case:

$$Z_2 = \frac{\eta_L^2}{Z_3} = \frac{\eta_L^2}{\eta_H^2} Z_4 = \left(\frac{n_H}{n_L}\right)^2 Z_4 = \left(\frac{n_H}{n_L}\right)^4 Z_6 = \left(\frac{n_H}{n_L}\right)^6 Z_8 = \left(\frac{n_H}{n_L}\right)^8 \eta_b$$

Therefore, after each bilayer, the impedance decreases by a factor of $(n_L/n_H)^2$. After N bilayers, we will have:

$$Z_2 = \left(\frac{n_H}{n_L}\right)^{2N} \eta_b \tag{6.3.2}$$

Using $Z_1 = \eta_H^2/Z_2$, we find for the reflection response at λ_0:

$$\Gamma_1 = \frac{Z_1 - \eta_a}{Z_1 + \eta_a} = \frac{1 - \left(\frac{n_H}{n_L}\right)^{2N} \frac{n_H^2}{n_a n_b}}{1 + \left(\frac{n_H}{n_L}\right)^{2N} \frac{n_H^2}{n_a n_b}} \tag{6.3.3}$$

It follows that for large N, Γ_1 will tend to -1, that is, 100% reflection.

Example 6.3.1: For nine layers, $2N + 1 = 9$, or $N = 4$, and $n_H = 2.32$, $n_L = 1.38$, and $n_a = n_b = 1$, we find:

$$\Gamma_1 = \frac{1 - \left(\frac{2.32}{1.38}\right)^8 2.32^2}{1 + \left(\frac{2.32}{1.38}\right)^8 2.32^2} = -0.9942 \quad \Rightarrow \quad |\Gamma_1|^2 = 98.84 \text{ percent}$$

For $N = 8$, or 17 layers, we have $\Gamma_1 = -0.9999$ and $|\Gamma_1|^2 = 99.98$ percent. If the substrate is glass with $n_b = 1.52$, the reflectances change to $|\Gamma_1|^2 = 98.25$ percent for $N = 4$, and $|\Gamma_1|^2 = 99.97$ percent for $N = 8$. □

To determine the bandwidth around λ_0 for which the structure exhibits high reflectivity, we work with the layer recursions (6.1.2). Because the bilayers are identical, the forward/backward fields at the left of one bilayer are related to those at the left of the next one by a transition matrix F, which is the product of two propagation matrices of the type of Eq. (6.1.2). The repeated application of the matrix F takes us to the right-most layer. For example, in Fig. 6.3.1 we have:

$$\begin{bmatrix} E_{2+} \\ E_{2-} \end{bmatrix} = F \begin{bmatrix} E_{4+} \\ E_{4-} \end{bmatrix} = F^2 \begin{bmatrix} E_{6+} \\ E_{6-} \end{bmatrix} = F^3 \begin{bmatrix} E_{8+} \\ E_{8-} \end{bmatrix} = F^4 \begin{bmatrix} E_{10+} \\ E_{10-} \end{bmatrix}$$

where F is the matrix:

$$F = \frac{1}{1+\rho}\begin{bmatrix} e^{jk_Ll_L} & \rho e^{-jk_Ll_L} \\ \rho e^{jk_Ll_L} & e^{-jk_Ll_L} \end{bmatrix}\frac{1}{1-\rho}\begin{bmatrix} e^{jk_Hl_H} & -\rho e^{-jk_Hl_H} \\ -\rho e^{jk_Hl_H} & e^{-jk_Hl_H} \end{bmatrix} \tag{6.3.4}$$

Defining the phase thicknesses $\delta_H = k_Hl_H$ and $\delta_L = k_Ll_L$, and multiplying the matrix factors out, we obtain the expression for F:

$$F = \frac{1}{1-\rho^2}\begin{bmatrix} e^{j(\delta_H+\delta_L)} - \rho^2 e^{j(\delta_H-\delta_L)} & -2j\rho e^{-j\delta_H}\sin\delta_L \\ 2j\rho e^{j\delta_H}\sin\delta_L & e^{-j(\delta_H+\delta_L)} - \rho^2 e^{-j(\delta_H-\delta_L)} \end{bmatrix} \tag{6.3.5}$$

By an additional transition matrix F_1 we can get to the left of interface-1 and by an additional matching matrix F_2 we pass to the right of the last interface:

$$\begin{bmatrix} E_{1+} \\ E_{1-} \end{bmatrix} = F_1\begin{bmatrix} E_{2+} \\ E_{2-} \end{bmatrix} = F_1F^4\begin{bmatrix} E_{10+} \\ E_{10-} \end{bmatrix} = F_1F^4F_2\begin{bmatrix} E'_{10+} \\ 0 \end{bmatrix}$$

where F_1 and F_2 are:

$$F_1 = \frac{1}{\tau_1}\begin{bmatrix} e^{jk_Hl_H} & \rho_1 e^{-jk_Hl_H} \\ \rho_1 e^{jk_Hl_H} & e^{-jk_Hl_H} \end{bmatrix}, \quad F_2 = \frac{1}{\tau_2}\begin{bmatrix} 1 & \rho_2 \\ \rho_2 & 1 \end{bmatrix} \tag{6.3.6}$$

where $\tau_1 = 1+\rho_1$, $\tau_2 = 1+\rho_2$, and ρ_1, ρ_2 were defined in Eq. (6.3.1). More generally, for $2N+1$ layers, or N bilayers, we have:

$$\begin{bmatrix} E_{2+} \\ E_{2-} \end{bmatrix} = F^N\begin{bmatrix} E_{2N+2,+} \\ E_{2N+2,-} \end{bmatrix}, \quad \begin{bmatrix} E_{1+} \\ E_{1-} \end{bmatrix} = F_1F^NF_2\begin{bmatrix} E'_{2N+2,+} \\ 0 \end{bmatrix} \tag{6.3.7}$$

Thus, the properties of the multilayer structure are essentially determined by the Nth power, F^N, of the bilayer transition matrix F. In turn, the behavior of F^N is determined by the eigenvalue structure of F.

Let $\{\lambda_+, \lambda_-\}$ be the two eigenvalues of F and let V be the eigenvector matrix. Then, the eigenvalue decomposition of F and F^N will be $F = V\Lambda V^{-1}$ and $F^N = V\Lambda^N V^{-1}$, where $\Lambda = \text{diag}\{\lambda_+, \lambda_-\}$. Because F has unit determinant, its two eigenvalues will be inverses of each other, that is, $\lambda_- = 1/\lambda_+$, or, $\lambda_+\lambda_- = 1$.

The eigenvalues $\lambda_\pm$ are either both real-valued or both complex-valued with unit magnitude. We can represent them in the equivalent form:

$$\lambda_+ = e^{jKl}, \quad \lambda_- = e^{-jKl} \tag{6.3.8}$$

where l is the length of each bilayer, $l = l_L + l_H$. The quantity K is referred to as the Bloch wavenumber. If the eigenvalues $\lambda_\pm$ are unit-magnitude complex-valued, then K is real. If the eigenvalues are real, then K is pure imaginary, say $K = -j\alpha$, so that $\lambda_\pm = e^{\pm jKl} = e^{\pm\alpha l}$.

The multilayer structure behaves very differently depending on the nature of K. The structure is primarily reflecting if K is imaginary and the eigenvalues $\lambda_\pm$ are real, and it is primarily transmitting if K is real and the eigenvalues are pure phases. To see this, we write Eq. (6.3.7) in the form:

$$\begin{bmatrix} E_{2+} \\ E_{2-} \end{bmatrix} = V\Lambda^NV^{-1}\begin{bmatrix} E_{2N+2,+} \\ E_{2N+2,-} \end{bmatrix} \quad \Rightarrow \quad V^{-1}\begin{bmatrix} E_{2+} \\ E_{2-} \end{bmatrix} = \Lambda^NV^{-1}\begin{bmatrix} E_{2N+2,+} \\ E_{2N+2,-} \end{bmatrix}, \quad \text{or,}$$

$$\begin{bmatrix} V_{2+} \\ V_{2-} \end{bmatrix} = \Lambda^N\begin{bmatrix} V_{2N+2,+} \\ V_{2N+2,-} \end{bmatrix}$$

where we defined

$$\begin{bmatrix} V_{2+} \\ V_{2-} \end{bmatrix} = V^{-1}\begin{bmatrix} E_{2+} \\ E_{2-} \end{bmatrix}, \quad \begin{bmatrix} V_{2N+2,+} \\ V_{2N+2,-} \end{bmatrix} = V^{-1}\begin{bmatrix} E_{2N+2,+} \\ E_{2N+2,-} \end{bmatrix}$$

We have $V_{2+} = \lambda_+^N V_{2N+2,+}$ and $V_{2-} = \lambda_-^N V_{2N+2,-} = \lambda_+^{-N} V_{2N+2,-}$ because Λ^N is diagonal. Thus,

$$V_{2N+2,+} = \lambda_+^{-N}V_{2+} = e^{-jKNl}V_{2+}, \quad V_{2N+2,-} = \lambda_+^N V_{2-} = e^{jKNl}V_{2-} \tag{6.3.9}$$

The quantity Nl is recognized as the total length of the bilayer structure, as depicted in Fig. 6.3.1. It follows that if K is real, the factor $\lambda_+^{-N} = e^{-jKNl}$ acts as a propagation phase factor and the fields transmit through the structure.

On the other hand, if K is imaginary, we have $\lambda_+^{-N} = e^{-\alpha Nl}$ and the fields attenuate exponentially as they propagate into the structure. In the limit of large N, the transmitted fields attenuate completely and the structure becomes 100% reflecting. For finite but large N, the structure will be mostly reflecting.

The eigenvalues $\lambda_\pm$ switch from real to complex, as K switches from imaginary to real, for certain frequency or wavenumber bands. The edges of these bands determine the bandwidths over which the structure will act as a mirror.

The eigenvalues are determined from the characteristic polynomial of F, given by the following expression which is valid for any 2×2 matrix:

$$\det(F - \lambda I) = \lambda^2 - (\text{tr}\,F)\lambda + \det F \tag{6.3.10}$$

where I is the 2×2 identity matrix. Because (6.3.5) has unit determinant, the eigenvalues are the solutions of the quadratic equation:

$$\lambda^2 - (\text{tr}\,F)\lambda + 1 = \lambda^2 - 2a\lambda + 1 = 0 \tag{6.3.11}$$

where we defined $a = (\text{tr}\,F)/2$. The solutions are:

$$\lambda_\pm = a \pm \sqrt{a^2 - 1} \tag{6.3.12}$$

where it follows from Eq. (6.3.5) that a is given by:

$$\boxed{a = \frac{1}{2}\text{tr}\,F = \frac{\cos(\delta_H+\delta_L) - \rho^2\cos(\delta_H-\delta_L)}{1-\rho^2}} \tag{6.3.13}$$

Using $\lambda_+ = e^{jKl} = a + \sqrt{a^2-1} = a + j\sqrt{1-a^2}$, we also find:

$$\boxed{a = \cos Kl \quad \Rightarrow \quad K = \frac{1}{l}\,\text{acos}(a)} \tag{6.3.14}$$

The sign of the quantity $a^2 - 1$ determines whether the eigenvalues are real or complex. The eigenvalues switch from real to complex—equivalently, K switches from imaginary to real—when $a^2 = 1$, or, $a = \pm 1$. These critical values of K are found from Eq. (6.3.14) to be:

$$K = \frac{1}{l}\,\text{acos}(\pm 1) = \frac{m\pi}{l} \tag{6.3.15}$$

where m is an integer. The lowest value is $K = \pi/l$ and corresponds to $a = -1$ and to $\lambda_+ = e^{jKl} = e^{j\pi} = -1$. Thus, we obtain the bandedge condition:

$$a = \frac{\cos(\delta_H + \delta_L) - \rho^2 \cos(\delta_H - \delta_L)}{1 - \rho^2} = -1$$

It can be manipulated into:

$$\boxed{\cos^2\left(\frac{\delta_H + \delta_L}{2}\right) = \rho^2 \cos^2\left(\frac{\delta_H - \delta_L}{2}\right)} \tag{6.3.16}$$

The dependence on the free-space wavelength λ or frequency $f = c_0/\lambda$ comes through $\delta_H = 2\pi(n_H l_H)/\lambda$ and $\delta_L = 2\pi(n_L l_L)/\lambda$. The solutions of (6.3.16) in λ determine the left and right bandedges of the reflecting regions.

These solutions can be obtained numerically with the help of the MATLAB function `omniband`, discussed in Sec. 8.8. An approximate solution, which is exact in the case of quarter-wave layers, is given below.

If the high and low index layers have equal optical thicknesses, $n_H l_H = n_L l_L$, such as when they are quarter-wavelength layers, or when the optical lengths are approximately equal, we can make the approximation $\cos\left((\delta_H - \delta_L)/2\right) = 1$. Then, (6.3.16) simplifies into:

$$\cos^2\left(\frac{\delta_H + \delta_L}{2}\right) = \rho^2 \tag{6.3.17}$$

with solutions:

$$\cos\left(\frac{\delta_H + \delta_L}{2}\right) = \pm\rho \quad \Rightarrow \quad \frac{\delta_H + \delta_L}{2} = \frac{\pi(n_H l_H + n_L l_L)}{\lambda} = \text{acos}(\pm\rho)$$

The solutions for the left and right bandedges and the bandwidth in λ are:

$$\lambda_1 = \frac{\pi(n_H l_H + n_L l_L)}{\text{acos}(-\rho)}, \quad \lambda_2 = \frac{\pi(n_H l_H + n_L l_L)}{\text{acos}(\rho)}, \quad \Delta\lambda = \lambda_2 - \lambda_1 \tag{6.3.18}$$

Similarly, the left/right bandedges in frequency are $f_1 = c_0/\lambda_2$ and $f_2 = c_0/\lambda_1$:

$$f_1 = c_0\,\frac{\text{acos}(\rho)}{\pi(n_H l_H + n_L l_L)}, \quad f_2 = c_0\,\frac{\text{acos}(-\rho)}{\pi(n_H l_H + n_L l_L)} \tag{6.3.19}$$

Noting that $\text{acos}(-\rho) = \pi/2 + \text{asin}(\rho)$ and $\text{acos}(\rho) = \pi/2 - \text{asin}(\rho)$, the frequency bandwidth can be written in the equivalent forms:

$$\Delta f = f_2 - f_1 = c_0\,\frac{\text{acos}(-\rho) - \text{acos}(\rho)}{\pi(n_H l_H + n_L l_L)} = c_0\,\frac{2\,\text{asin}(\rho)}{\pi(n_H l_H + n_L l_L)} \tag{6.3.20}$$

Relative to some desired wavelength $\lambda_0 = c_0/f_0$, the normalized bandwidths in wavelength and frequency are:

$$\frac{\Delta\lambda}{\lambda_0} = \frac{\pi(n_H l_H + n_L l_L)}{\lambda_0}\left[\frac{1}{\text{acos}(\rho)} - \frac{1}{\text{acos}(-\rho)}\right] \tag{6.3.21}$$

$$\frac{\Delta f}{f_0} = \frac{2\lambda_0\,\text{asin}(\rho)}{\pi(n_H l_H + n_L l_L)} \tag{6.3.22}$$

Similarly, the center of the reflecting band $f_c = (f_1 + f_2)/2$ is:

$$\frac{f_c}{f_0} = \frac{\lambda_0}{2(n_H l_H + n_L l_L)} \tag{6.3.23}$$

If the layers have equal quarter-wave optical lengths at λ_0, that is, $n_H l_H = n_L l_L = \lambda_0/4$, then, $f_c = f_0$ and the matrix F takes the simplified form:

$$F = \frac{1}{1-\rho^2}\begin{bmatrix} e^{2j\delta} - \rho^2 & -2j\rho e^{-j\delta}\sin\delta \\ 2j\rho e^{j\delta}\sin\delta & e^{-2j\delta} - \rho^2 \end{bmatrix} \tag{6.3.24}$$

where $\delta = \delta_H = \delta_L = 2\pi(n_H l_H)/\lambda = 2\pi(\lambda_0/4)/\lambda = (\pi/2)\lambda_0/\lambda = (\pi/2)f/f_0$. Then, Eqs. (6.3.21) and (6.3.22) simplify into:

$$\frac{\Delta\lambda}{\lambda_0} = \frac{\pi}{2}\left[\frac{1}{\text{acos}(\rho)} - \frac{1}{\text{acos}(-\rho)}\right], \quad \frac{\Delta f}{f_0} = \frac{4}{\pi}\,\text{asin}(\rho) \tag{6.3.25}$$

Example 6.3.2: *Dielectric Mirror With Quarter-Wavelength Layers.* Fig. 6.3.2 shows the reflection response $|\Gamma_1|^2$ as a function of the free-space wavelength λ and as a function of frequency $f = c_0/\lambda$. The high and low indices are $n_H = 2.32$ and $n_L = 1.38$, corresponding to zinc sulfide (ZnS) and magnesium fluoride. The incident medium is air and the substrate is glass with indices $n_a = 1$ and $n_b = 1.52$. The left graph depicts the response for the cases of $N = 2, 4, 8$ bilayers, or $2N + 1 = 5, 9, 17$ layers, as defined in Fig. 6.3.1. The design wavelength at which the layers are quarter-wavelength long is $\lambda_0 = 500$ nm.

The reflection coefficient is $\rho = 0.25$ and the ratio $n_H/n_L = 1.68$. The wavelength bandwidth calculated from Eq. (6.3.25) is $\Delta\lambda = 168.02$ nm and has been placed on the graph at an arbitrary reflectance level. The left/right bandedges are $\lambda_1 = 429.73$, $\lambda_2 = 597.75$ nm. The bandwidth covers most of the visible spectrum. As the number of bilayers N increases, the reflection response becomes flatter within the bandwidth $\Delta\lambda$, and has sharper edges and tends to 100%. The bandwidth $\Delta\lambda$ represents the asymptotic width of the reflecting band.

The right figure depicts the reflection response as a function of frequency f and is plotted in the normalized variable f/f_0. Because the phase thickness of each layer is $\delta = \pi f/2f_0$ and the matrix F is periodic in δ, the mirror behavior of the structure will occur at odd multiples of f_0 (or odd multiples of $\pi/2$ for δ.) As discussed in Sec. 6.6, the structure acts as a sampled system with sampling frequency $f_s = 2f_0$, and therefore, $f_0 = f_s/2$ plays the role of the Nyquist frequency.

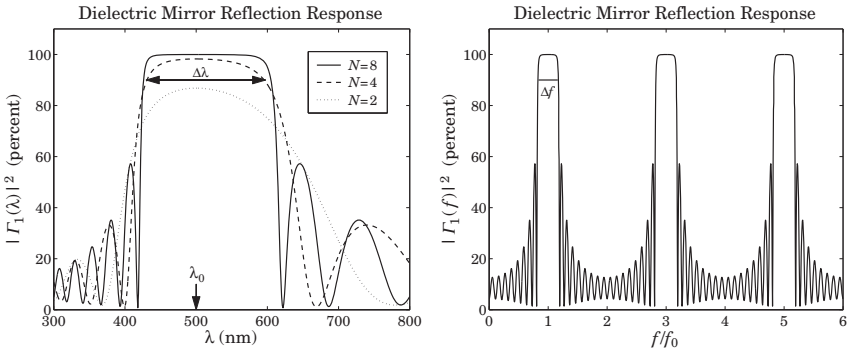

Fig. 6.3.2 Dielectric mirror with quarter-wavelength layers.

The typical MATLAB code used to generate these graphs was:

```
na = 1; nb = 1.52; nH = 2.32; nL = 1.38;      % refractive indices
LH = 0.25; LL = 0.25;                         % optical thicknesses in units of λ0
la0 = 500;                                    % λ0 in units of nm

rho = (nH-nL)/(nH+nL);                        % reflection coefficient ρ

la2 = pi*(LL+LH)*1/acos(rho) * la0;           % right bandedge
la1 = pi*(LL+LH)*1/acos(-rho) * la0;          % left bandedge
Dla = la2-la1;                                % bandwidth

N = 8;                                        % number of bilayers
n = [na, nH, repmat([nL,nH], 1, N), nb];      % indices for the layers A|H(LH)^N|G
L = [LH, repmat([LL,LH], 1, N)];              % lengths of the layers H(LH)^N

la = linspace(300,800,501);                   % plotting range is 300 ≤ λ ≤ 800 nm
Gla = 100*abs(multidiel(n,L,la/la0)).^2;      % reflectance as a function of λ
figure; plot(la,Gla);

f = linspace(0,6,1201);                       % frequency plot over 0 ≤ f ≤ 6f0
Gf = 100*abs(multidiel(n,L,1./f)).^2;         % reflectance as a function of f
figure; plot(f,Gf);
```

Note that the function `repmat` replicates the LH bilayer N times. The frequency graph shows only the case of $N = 8$. The bandwidth Δf, calculated from (6.3.25), has been placed on the graph. The maximum reflectance (evaluated at odd multiples of f_0) is equal to 99.97%. □

Example 6.3.3: *Dielectric Mirror with Unequal-Length Layers.* Fig. 6.3.3 shows the reflection response of a mirror having unequal optical lengths for the high and low index films.

The parameters of this example correspond very closely to the recently constructed omnidirectional dielectric mirror [777], which was designed to be a mirror over the infrared band of 10–15 μm. The number of layers is nine and the number of bilayers, $N = 4$. The indices of refraction are $n_H = 4.6$ and $n_L = 1.6$ corresponding to Tellurium and Polystyrene.

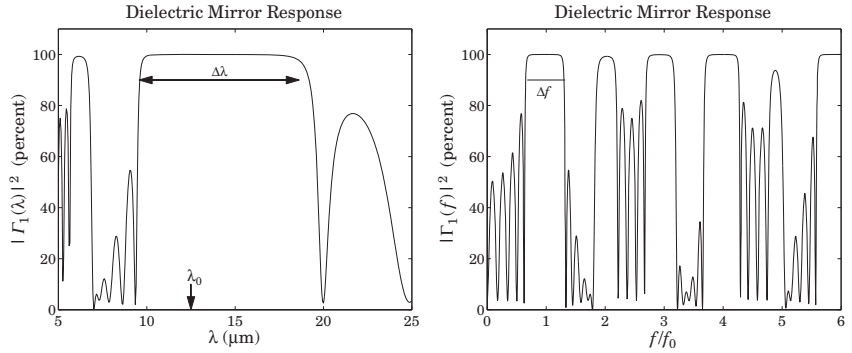

Fig. 6.3.3 Dielectric mirror with unequal optical thicknesses.

Their ratio is $n_H/n_L = 2.875$ and the reflection coefficient, $\rho = 0.48$. The incident medium and substrate are air and NaCl ($n = 1.48$.)

The center wavelength is taken to be at the middle of the 10–15 μm band, that is, $\lambda_0 = 12.5$ μm. The lengths of the layers are $l_H = 0.8$ and $l_L = 1.65$ μm, resulting in the optical lengths (relative to λ_0) $n_H l_H = 0.2944\lambda_0$ and $n_L l_L = 0.2112\lambda_0$. The wavelength bandwidth, calculated from Eq. (6.3.21), is $\Delta\lambda = 9.07$ μm. The typical MATLAB code for generating the figures of this example was as follows:

```
la0 = 12.5;
na = 1; nb = 1.48;                            % NaCl substrate
nH = 4.6; nL = 1.6;                           % Te and PS
lH = 0.8; lL = 1.65;                          % physical lengths lH, lL
LH = nH*lH/la0, LL = nL*lL/la0;               % optical lengths in units of λ0

rho = (nH-nL)/(nH+nL);                        % reflection coefficient ρ

la2 = pi*(LL+LH)*1/acos(rho) * la0;           % right bandedge
la1 = pi*(LL+LH)*1/acos(-rho) * la0;          % left bandedge
Dla = la2-la1;                                % bandwidth

la = linspace(5,25,401);                      % equally-spaced wavelengths

N = 4;
n = [na, nH, repmat([nL,nH], 1, N), nb];      % refractive indices of all media
L = [LH, repmat([LL,LH], 1, N)];              % optical lengths of the slabs
G = 100 * abs(multidiel(n,L,la/la0)).^2;      % reflectance

plot(la,G);
```

The bandwidth $\Delta\lambda$ shown on the graph is wider than that of the omnidirectional mirror presented in [777], because our analysis assumes normal incidence only. The condition for omnidirectional reflectivity for both TE and TM modes causes the bandwidth to narrow by about half of what is shown in the figure. The reflectance as a function of frequency is no longer periodic at odd multiples of f_0 because the layers have lengths that are not equal to $\lambda_0/4$. The omnidirectional case is discussed in Example 8.8.3.

The maximum reflectivity achieved within the mirror bandwidth is 99.99%, which is better than that of the previous example with 17 layers. This can be explained because the ratio n_H/n_L is much larger here. □

Although the reflectances in the previous two examples were computed with the help of the MATLAB function `multidiel`, it is possible to derive closed-form expressions for Γ_1 that are valid for any number of bilayers N. Applying Eq. (6.1.3) to interface-1 and interface-2, we have:

$$\Gamma_1 = \frac{\rho_1 + e^{-2j\delta_H}\Gamma_2}{1 + \rho_1 e^{-2j\delta_H}\Gamma_2} \tag{6.3.26}$$

where $\Gamma_2 = E_{2-}/E_{2+}$, which can be computed from the matrix equation (6.3.7). Thus, we need to obtain a closed-form expression for Γ_2.

It is a general property of any 2×2 unimodular matrix F that its Nth power can be obtained from the following simple formula, which involves the Nth powers of its eigenvalues $\lambda_\pm$:†

$$F^N = \left(\frac{\lambda_+^N - \lambda_-^N}{\lambda_+ - \lambda_-}\right) F - \left(\frac{\lambda_+^{N-1} - \lambda_-^{N-1}}{\lambda_+ - \lambda_-}\right) I = W_N F - W_{N-1} I \tag{6.3.27}$$

where $W_N = (\lambda_+^N - \lambda_-^N)/(\lambda_+ - \lambda_-)$. To prove it, we note that the formula holds as a simple identity when F is replaced by its diagonal version $\Lambda = \text{diag}\{\lambda_+, \lambda_-\}$:

$$\Lambda^N = \left(\frac{\lambda_+^N - \lambda_-^N}{\lambda_+ - \lambda_-}\right) \Lambda - \left(\frac{\lambda_+^{N-1} - \lambda_-^{N-1}}{\lambda_+ - \lambda_-}\right) I \tag{6.3.28}$$

Eq. (6.3.27) then follows by multiplying (6.3.28) from left and right by the eigenvector matrix V and using $F = V\Lambda V^{-1}$ and $F^N = V\Lambda^N V^{-1}$. Defining the matrix elements of F and F^N by

$$F = \begin{bmatrix} A & B \\ B^* & A^* \end{bmatrix}, \quad F^N = \begin{bmatrix} A_N & B_N \\ B_N^* & A_N^* \end{bmatrix}, \tag{6.3.29}$$

it follows from (6.3.27) that:

$$A_N = AW_N - W_{N-1}\,, \quad B_N = BW_N \tag{6.3.30}$$

where we defined:

$$A = \frac{e^{j(\delta_H+\delta_L)} - \rho^2 e^{j(\delta_H-\delta_L)}}{1-\rho^2}\,, \quad B = -\frac{2j\rho e^{-j\delta_H}\sin\delta_L}{1-\rho^2} \tag{6.3.31}$$

Because F and F^N are unimodular, their matrix elements satisfy the conditions:

$$|A|^2 - |B|^2 = 1\,, \quad |A_N|^2 - |B_N|^2 = 1 \tag{6.3.32}$$

The first follows directly from the definition (6.3.29), and the second can be verified easily. It follows now that the product $F^N F_2$ in Eq. (6.3.7) is:

†The coefficients W_N are related to the Chebyshev polynomials of the second kind $U_m(x)$ through $W_N = U_{N-1}(a) = \sin\big(N\arccos(a)\big)/\sqrt{1-a^2} = \sin(NKl)/\sin(Kl)$.

$$F^N F_2 = \frac{1}{\tau_2}\begin{bmatrix} A_N + \rho_2 B_N & B_N + \rho_2 A_N \\ B_N^* + \rho_2 A_N^* & A_N^* + \rho_2 B_N^* \end{bmatrix}$$

Therefore, the desired closed-form expression for the reflection coefficient Γ_2 is:

$$\Gamma_2 = \frac{B_N^* + \rho_2 A_N^*}{A_N + \rho_2 B_N} = \frac{B^* W_N + \rho_2 (A^* W_N - W_{N-1})}{AW_N - W_{N-1} + \rho_2 B W_N} \tag{6.3.33}$$

Suppose now that $a^2 < 1$ and the eigenvalues are pure phases. Then, W_N are oscillatory as functions of the wavelength λ or frequency f and the structure will transmit.

On the other hand, if f lies in the mirror bands, so that $a^2 > 1$, then the eigenvalues will be real with $|\lambda_+| > 1$ and $|\lambda_-| < 1$. In the limit of large N, W_N and W_{N-1} will behave like:

$$W_N \to \frac{\lambda_+^N}{\lambda_+ - \lambda_-}\,, \quad W_{N-1} \to \frac{\lambda_+^{N-1}}{\lambda_+ - \lambda_-}$$

In this limit, the reflection coefficient Γ_2 becomes:

$$\Gamma_2 \to \frac{B^* + \rho_2 (A^* - \lambda_+^{-1})}{A - \lambda_+^{-1} + \rho_2 B} \tag{6.3.34}$$

where we canceled some common diverging factors from all terms. Using conditions (6.3.32) and the eigenvalue equation (6.3.11), and recognizing that $\text{Re}(A) = a$, it can be shown that this asymptotic limit of Γ_2 is unimodular, $|\Gamma_2| = 1$, regardless of the value of ρ_2.

This immediately implies that Γ_1 given by Eq. (6.3.26) will also be unimodular, $|\Gamma_1| = 1$, regardless of the value of ρ_1. In other words, the structure tends to become a perfect mirror as the number of bilayers increases.

Next, we discuss some variations on dielectric mirrors that result in (a) multiband mirrors and (b) longpass and shortpass filters that pass long or short wavelengths, in analogy with lowpass and highpass filters that pass low or high frequencies.

Example 6.3.4: *Multiband Reflectors.* The quarter-wave stack of bilayers of Example 6.3.2 can be denoted compactly as $AH(LH)^8G$ (for the case $N = 8$), meaning 'air', followed by a "high-index" quarter-wave layer, followed by four "low/high" bilayers, followed by the "glass" substrate.

Similarly, Example 6.3.3 can be denoted by $A(1.18H)(0.85L\,1.18H)^4G$, where the layer optical lengths have been expressed in units of $\lambda_0/4$, that is, $n_L l_L = 0.85(\lambda_0/4)$ and $n_H l_H = 1.18(\lambda_0/4)$.

Another possibility for a periodic bilayer structure is to replace one or both of the L or H layers by integral multiples thereof [636]. Fig. 6.3.4 shows two such examples. In the first, each H layer has been replaced by a half-wave layer, that is, two quarter-wave layers $2H$, so that the total structure is $A(2H)(L\,2H)^8G$, where n_a,n_b,n_H,n_L are the same as in Example 6.3.2. In the second case, each H has been replaced by a three-quarter-wave layer, resulting in $A(3H)(L\,3H)^8G$.

The mirror peaks at odd multiples of f_0 of Example 6.3.2 get split into two or three peaks each. □

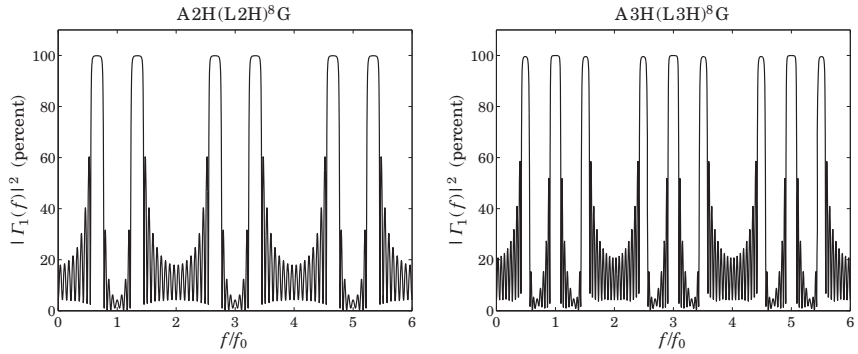

Fig. 6.3.4 Dielectric mirrors with split bands.

Example 6.3.5: *Shortpass and Longpass Filters.* By adding an eighth-wave low-index layer, that is, a $(0.5L)$, at both ends of Example 6.3.2, we can decrease the reflectivity of the short wavelengths. Thus, the stack $AH(LH)^8G$ is replaced by $A(0.5L)H(LH)^8(0.5L)G$.

For example, suppose we wish to have high reflectivity over the $[600, 700]$ nm range and low reflectivity below 500 nm. The left graph in Fig. 6.3.5 shows the resulting reflectance with the design wavelength chosen to be $\lambda_0 = 650$ nm. The parameters n_a, n_b, n_H, n_L are the same as in Example 6.3.2

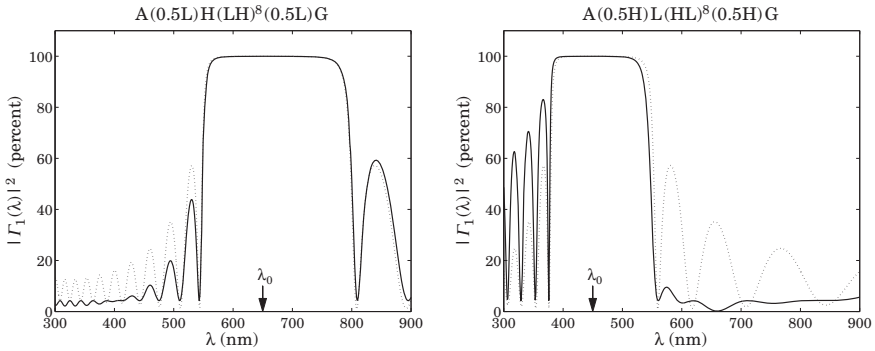

Fig. 6.3.5 Short- and long-pass wavelength filters.

The right graph of Fig. 6.3.5 shows the stack $A(0.5H)L(HL)^8(0.5H)G$ obtained from the previous case by *interchanging* the roles of H and L. Now, the resulting reflectance is low for the higher wavelengths. The design wavelength was chosen to be $\lambda_0 = 450$ nm. It can be seen from the graph that the reflectance is high within the band $[400, 500]$ nm and low above 600 nm.

Superimposed on both graphs is the reflectance of the original $AH(LH)^8G$ stack centered at the corresponding λ_0 (dotted curves.)

Both of these examples can also be thought of as the periodic repetition of a symmetric triple layer of the form $A(BCB)^NG$. Indeed, we have the equivalences:

$$A(0.5L)H(LH)^8(0.5L)G = A(0.5L\,H\,0.5L)^9G$$

$$A(0.5H)L(HL)^8(0.5H)G = A(0.5H\,L\,0.5H)^9G$$

The symmetric triple combination BCB can be replaced by an *equivalent single layer*, which facilitates the analysis of such structures [634,662–664,666]. □

6.4 Propagation Bandgaps

There is a certain analogy between the electronic energy bands of solid state materials arising from the periodicity of the crystal structure and the frequency bands of dielectric mirrors arising from the periodicity of the bilayers. The high-reflectance bands play the role of the forbidden energy bands (in the sense that waves cannot propagate through the structure in these bands.) Such periodic dielectric structures have been termed *photonic crystals* and have given rise to the new field of *photonic bandgap structures*, which has grown rapidly over the past ten years with a large number of potential novel applications [761–787].

Propagation bandgaps arise in any wave propagation problem in a medium with periodic structure [754–760]. Waveguides and transmission lines that are periodically loaded with ridges or shunt impedances, are examples of such media [884–888].

Fiber Bragg gratings, obtained by periodically modulating the refractive index of the core (or the cladding) of a finite portion of a fiber, exhibit high reflectance bands [788–808]. Quarter-wave phase-shifted fiber Bragg gratings (discussed in the next section) act as narrow-band transmission filters and can be used in wavelength multiplexed communications systems.

Other applications of periodic structures with bandgaps arise in structural engineering for the control of vibration transmission and stress [809–811], in acoustics for the control of sound transmission through structures [812–817], and in the construction of laser resonators and periodic lens systems [913,915]. A nice review of wave propagation in periodic structures can be found in [755].

6.5 Narrow-Band Transmission Filters

The reflection bands of a dielectric mirror arise from the N-fold periodic replication of high/low index layers of the type $(HL)^N$, where H, L can have arbitrary lengths. Here, we will assume that they are quarter-wavelength layers at the design wavelength λ_0.

A quarter-wave phase-shifted multilayer structure is obtained by doubling $(HL)^N$ to $(HL)^N(HL)^N$ and then inserting a quarter-wave layer L between the two groups, resulting in $(HL)^NL(HL)^N$. We are going to refer to such a structure as a *Fabry-Perot resonator* (FPR)—it can also be called a *quarter-wave phase-shifted Bragg grating.*

An FPR behaves like a single L-layer at the design wavelength λ_0. Indeed, noting that at λ_0 the combinations LL and HH are half-wave or absentee layers and can be deleted, we obtain the successive reductions:

$$\begin{aligned}(HL)^N L(HL)^N &\rightarrow (HL)^{N-1}HLLHL(HL)^{N-1}\\ &\rightarrow (HL)^{N-1}HHL(HL)^{N-1}\\ &\rightarrow (HL)^{N-1}L(HL)^{N-1}\end{aligned}$$

Thus, the number of the HL layers can be successively reduced, eventually resulting in the equivalent layer L (at λ_0):

$$(HL)^N L(HL)^N \rightarrow (HL)^{N-1}L(HL)^{N-1} \rightarrow (HL)^{N-2}L(HL)^{N-2} \rightarrow \cdots \rightarrow L$$

Adding another L-layer on the right, the structure $(HL)^N L(HL)^N L$ will act as $2L$, that is, a half-wave absentee layer at λ_0. If such a structure is sandwiched between the same substrate material, say glass, then it will act as an absentee layer, opening up a narrow transmission window at λ_0, in the middle of its reflecting band.

Without the quarter-wave layers L present, the structures $G|(HL)^N(HL)^N|G$ and $G|(HL)^N|G$ act as mirrors,[†] but with the quarter-wave layers present, the structure $G|(HL)^N L(HL)^N L|G$ acts as a narrow transmission filter, with the transmission bandwidth becoming narrower as N increases.

By repeating the FPR $(HL)^N L(HL)^N$ several times and using possibly different lengths N, it is possible to design a very narrow transmission band centered at λ_0 having a flat passband and very sharp edges.

Thus, we arrive at a whole family of designs, where starting with an ordinary dielectric mirror, we may replace it with one, two, three, four, and so on, FPRs:

$$\begin{aligned}&0.\quad G|(HL)^{N_1}|G\\ &1.\quad G|(HL)^{N_1}L(HL)^{N_1}|L|G\\ &2.\quad G|(HL)^{N_1}L(HL)^{N_1}|(HL)^{N_2}L(HL)^{N_2}|G\\ &3.\quad G|(HL)^{N_1}L(HL)^{N_1}|(HL)^{N_2}L(HL)^{N_2}|(HL)^{N_3}L(HL)^{N_3}|L|G\\ &4.\quad G|(HL)^{N_1}L(HL)^{N_1}|(HL)^{N_2}L(HL)^{N_2}|(HL)^{N_3}L(HL)^{N_3}|(HL)^{N_4}L(HL)^{N_4}|G\end{aligned} \tag{6.5.1}$$

Note that when an odd number of FPRs $(HL)^N L(HL)^N$ are used, an extra L layer must be added at the end to make the overall structure absentee. For an even number of FPRs, this is not necessary.

Such filter designs have been used in thin-film applications [637–643] and in fiber Bragg gratings, for example, as demultiplexers for WDM systems and for generating very-narrow-bandwidth laser sources (typically at $\lambda_0 = 1550$ nm) with distributed feedback lasers [798–808]. We discuss fiber Bragg gratings in Sec. 12.4.

In a Fabry-Perot interferometer, the quarter-wave layer L sandwiched between the mirrors $(HL)^N$ is called a "spacer" or a "cavity" and can be replaced by any odd multiple of quarter-wave layers, for example, $(HL)^N(5L)(HL)^N$.

[†] G denotes the glass substrate.

Several variations of FPR filters are possible, such as interchanging the role of H and L, or using symmetric structures. For example, using eighth-wave layers $L/2$, the following symmetric multilayer structure will also act like as a single L at λ_0:

$$\left(\frac{L}{2}H\frac{L}{2}\right)^N L \left(\frac{L}{2}H\frac{L}{2}\right)^N$$

To create an absentee structure, we may sandwich this between two $L/2$ layers:

$$\frac{L}{2}\left(\frac{L}{2}H\frac{L}{2}\right)^N L \left(\frac{L}{2}H\frac{L}{2}\right)^N \frac{L}{2}$$

This can be seen to be equivalent to $(HL)^N(2L)(LH)^N$, which is absentee at λ_0. This equivalence follows from the identities:

$$\begin{aligned}\frac{L}{2}\left(\frac{L}{2}H\frac{L}{2}\right)^N &\equiv (LH)^N\frac{L}{2}\\ \left(\frac{L}{2}H\frac{L}{2}\right)^N\frac{L}{2} &\equiv \frac{L}{2}(HL)^N\end{aligned} \tag{6.5.2}$$

Example 6.5.1: *Transmission Filter Design with One FPR.* This example illustrates the basic transmission properties of FPR filters. We choose parameters that might closely emulate the case of a fiber Bragg grating for WDM applications. The refractive indices of the left and right substrates and the layers were: $n_a = n_b = 1.52$, $n_L = 1.4$, and $n_H = 2.1$. The design wavelength at which the layers are quarter wavelength is taken to be the standard laser source $\lambda_0 = 1550$ nm.

First, we compare the cases of a dielectric mirror $(HL)^N$ and its phase-shifted version using a single FPR (cases 0 and 1 in Eq. (6.5.1)), with number of layers $N_1 = 6$. Fig. 6.5.1 shows the transmittance, that is, the quantity $(1-|\Gamma_1(\lambda)|^2)$ plotted over the range $1200 \le \lambda \le 2000$ nm.

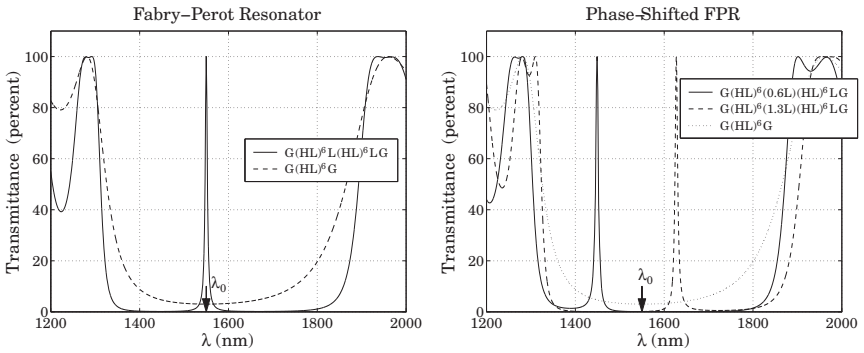

Fig. 6.5.1 Narrowband FPR transmission filters.

We observe that the mirror (case 0) has a suppressed transmittance over the entire reflecting band, whereas the FPR filter (case 1) has a narrow peak at λ_0. The asymptotic edges of

the reflecting band are calculated from Eq. (6.3.18) to be $\lambda_1 = 1373.9$ nm and $\lambda_2 = 1777.9$ nm, resulting in a width of $\Delta\lambda = 404$ nm. The MATLAB code used to generated the left graph was:

```
na = 1.52; nb = 1.52; nH = 2.1; nL = 1.4;
LH = 0.25; LL = 0.25;                                   % optical thicknesses

la0 = 1550;
la = linspace(1200, 2000, 8001);                        % 1200 ≤ λ ≤ 2000 nm

N1 = 6;

n1 = repmat([nH,nL],1,N1);
L1 = repmat([LH,LL],1,N1);
n = [na, n1, nb];
L = L1;
G0 = 100*(1 - abs(multidiel(n,L,la/la0)).^2);           % no phase shift

n1 = [repmat([nH,nL],1,N1), nL, repmat([nH,nL],1,N1)];
L1 = [repmat([LH,LL],1,N1), LL, repmat([LH,LL],1,N1)];
n = [na, n1, nL, nb];
L = [L1, LL];
G1 = 100*(1 - abs(multidiel(n,L,la/la0)).^2);           % one phase shift

plot(la,G1,la,G0);
```

The location of the peak can be shifted by making the phase-shift different from $\lambda/4$. This can be accomplished by changing the optical thickness of the middle L-layer to some other value. The right graph of Fig. 6.5.1 shows the two cases where that length was chosen to be $n_L l_L = (0.6)\lambda_0/4$ and $(1.3)\lambda_0/4$, corresponding to phase shifts of 54° and 117°. □

Example 6.5.2: *Transmission Filter Design with Two FPRs.* Fig. 6.5.2 shows the transmittance of a grating with two FPRs (case 2 of Eq. (6.5.1)). The number of bilayers were $N_1 = N_2 = 8$ in the first design, and $N_1 = N_2 = 9$ in the second.

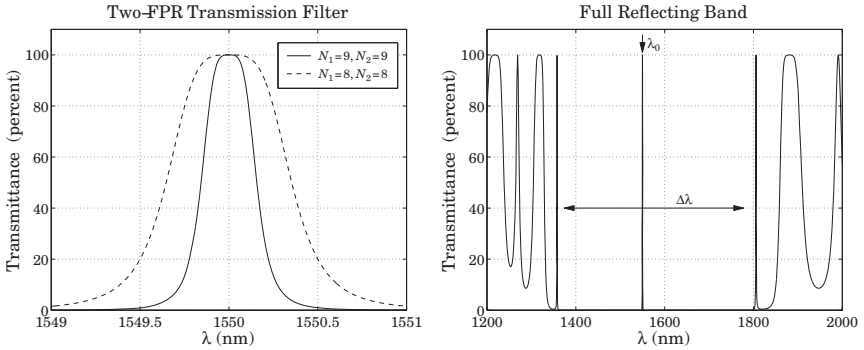

Fig. 6.5.2 Narrow-band transmission filter made with two FPRs.

The resulting transmittance bands are extremely narrow. The plotting scale is only from 1549 nm to 1551 nm. To see these bands in the context of the reflectance band, the

transmittance (for $N_1 = N_2 = 8$) is plotted on the right graph over the range $[1200, 2000]$ nm, which includes the full reflectance band of $[1373.9, 1777.9]$ nm.

Using two FPRs has the effect of narrowing the transmittance band and making it somewhat flatter at its top. □

Example 6.5.3: *Transmission Filter Design with Three and Four FPRs.* Fig. 6.5.3 shows the transmittance of a grating with three FPRs (case 3 of Eq. (6.5.1)). A symmetric arrangement of FPRs was chosen such that $N_3 = N_1$.

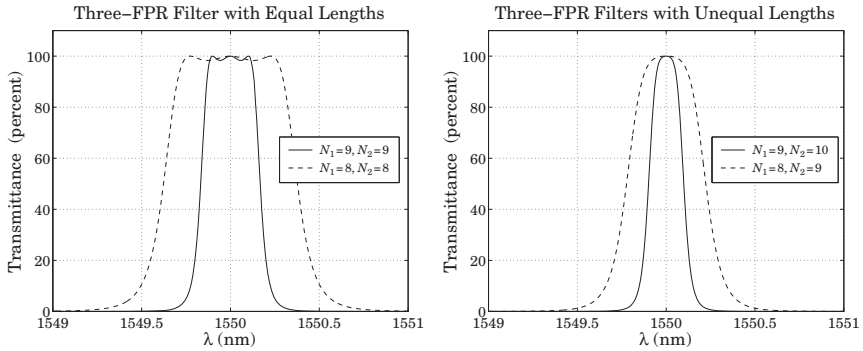

Fig. 6.5.3 Transmission filters with three FPRs of equal and unequal lengths.

The left graph shows the transmittances of the two design cases $N_1 = N_2 = N_3 = 8$ and $N_1 = N_2 = N_3 = 9$, so that all the FPRs have the same lengths. The transmission band is now flatter but exhibits some ripples. To get rid of the ripples, the length of the middle FPR is slightly increased. The right graph shows the case $N_1 = N_3 = 8$ and $N_2 = 9$, and the case $N_1 = N_3 = 9$ and $N_2 = 10$.

Fig. 6.5.4 shows the case of four FPRs (case 4 in Eq. (6.5.1).) Again, a symmetric arrangement was chosen with $N_1 = N_4$ and $N_2 = N_3$.

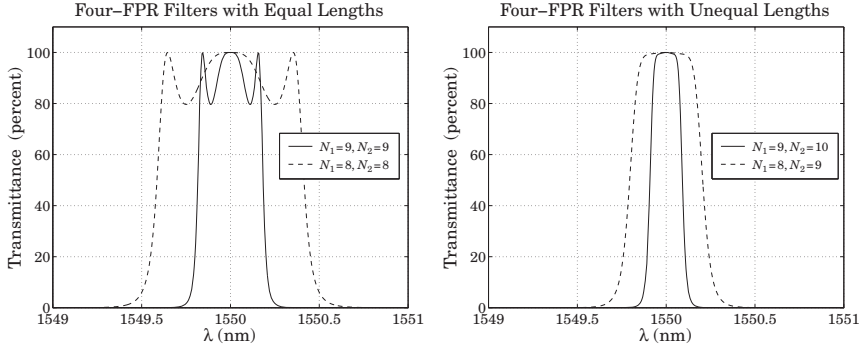

Fig. 6.5.4 Transmission filters with four FPRs of equal and unequal lengths.

The left graph shows the two cases of equal lengths $N_1 = N_2 = N_3 = N_4 = 8$ and $N_1 = N_2 = N_3 = N_4 = 9$. The right graphs shows the case $N_1 = N_4 = 8$ and $N_2 = N_4 = 9$, and the case $N_1 = N_4 = 9$ and $N_2 = N_3 = 10$. We notice again that the equal length cases exhibit ripples, but increasing the length of the middle FPRs tends to eliminate them. The typical MATLAB code for generating the case $N_1 = N_4 = 9$ and $N_2 = N_3 = 10$ was as follows:

```
na = 1.52; nb = 1.52; nH = 2.1; nL = 1.4;
LH = 0.25; LL = 0.25;
la0 = 1550;
la = linspace(1549, 1551, 501);

N1 = 9; N2 = 10; N3 = N2; N4 = N1;

n1 = [repmat([nH,nL],1,N1), nL, repmat([nH,nL],1,N1)];
n2 = [repmat([nH,nL],1,N2), nL, repmat([nH,nL],1,N2)];
n3 = [repmat([nH,nL],1,N3), nL, repmat([nH,nL],1,N3)];
n4 = [repmat([nH,nL],1,N4), nL, repmat([nH,nL],1,N4)];
L1 = [repmat([LH,LL],1,N1), LL, repmat([LH,LL],1,N1)];
L2 = [repmat([LH,LL],1,N2), LL, repmat([LH,LL],1,N2)];
L3 = [repmat([LH,LL],1,N3), LL, repmat([LH,LL],1,N3)];
L4 = [repmat([LH,LL],1,N4), LL, repmat([LH,LL],1,N4)];

n = [na, n1, n2, n3, n4, nb];
L = [L1, L2, L3, L4];

G = 100*(1 - abs(multidiel(n,L,la/la0)).^2);
plot(la,G);
```

The resulting transmittance band is fairly flat with a bandwidth of approximately 0.15 nm, as would be appropriate for dense WDM systems. The second design case with $N_1 = 8$ and $N_2 = 9$ has a bandwidth of about 0.3 nm.

The effect of the relative lengths N_1, N_2 on the shape of the transmittance band has been studied in [804–806]. The equivalence of the low/high multilayer dielectric structures to coupled-mode models of fiber Bragg gratings has been discussed in [795]. □

6.6 Equal Travel-Time Multilayer Structures

Here, we discuss the specialized, but useful, case of a multilayer structure whose layers have equal optical thicknesses, or equivalently, equal travel-time delays, as for example in the case of quarter-wavelength layers. Our discussion is based on [833] and on [840,841].

Fig. 6.6.1 depicts such a structure consisting of M layers. The media to the left and right are η_a and η_b and the reflection coefficients ρ_i at the $M+1$ interfaces are as in Eq. (6.1.1). We will discuss the general case when there are incident fields from both the left and right media.

Let T_s denote the common two-way travel-time delay, so that,

$$\frac{2n_1l_1}{c_0} = \frac{2n_2l_2}{c_0} = \cdots = \frac{2n_Ml_M}{c_0} = T_s \tag{6.6.1}$$

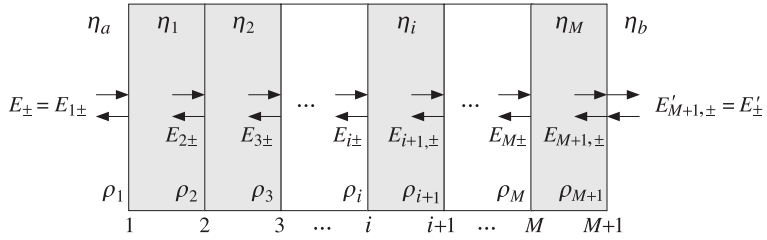

Fig. 6.6.1 Equal travel-time multilayer structure.

Then, all layers have a common phase thickness, that is, for $i = 1, 2, \ldots, M$:

$$\delta = k_il_i = \frac{\omega n_il_i}{c_0} = \frac{1}{2}\omega T_s \tag{6.6.2}$$

where we wrote $k_i = \omega/c_i = \omega n_i/c_0$. The layer recursions (6.1.2)–(6.1.5) simplify considerably in this case. These recursions and other properties of the structure can be described using DSP language.

Because the layers have a common roundtrip time delay T_s, the overall structure will act as a sampled system with sampling period T_s and sampling frequency $f_s = 1/T_s$. The corresponding "Nyquist frequency", $f_0 = f_s/2$, plays a special role. The phase thickness δ can be expressed in terms of f and f_0 as follows:

$$\delta = \frac{1}{2}\omega T_s = \frac{1}{2}2\pi f\frac{1}{f_s} = \pi\frac{f}{f_s} = \frac{\pi}{2}\frac{f}{f_0}$$

Therefore, at $f = f_0$ (and odd multiples thereof), the phase thickness will be $\pi/2 = (2\pi)/4$, that is, the structure will act as quarter-wave layers. Defining the z-domain variable:

$$\boxed{z = e^{2j\delta} = e^{j\omega T_s} = e^{2jk_il_i}} \tag{6.6.3}$$

we write Eq. (6.1.2) in the form:

$$\begin{bmatrix} E_{i+} \\ E_{i-} \end{bmatrix} = \frac{z^{1/2}}{\tau_i}\begin{bmatrix} 1 & \rho_iz^{-1} \\ \rho_i & z^{-1} \end{bmatrix}\begin{bmatrix} E_{i+1,+} \\ E_{i+1,-} \end{bmatrix}, \quad i = M, M-1, \ldots, 1 \tag{6.6.4}$$

We may rewrite it compactly as:

$$\mathbf{E}_i(z) = F_i(z)\mathbf{E}_{i+1}(z) \tag{6.6.5}$$

where we defined:

$$F_i(z) = \frac{z^{1/2}}{\tau_i}\begin{bmatrix} 1 & \rho_iz^{-1} \\ \rho_i & z^{-1} \end{bmatrix}, \qquad \mathbf{E}_i(z) = \begin{bmatrix} E_{i+}(z) \\ E_{i-}(z) \end{bmatrix} \tag{6.6.6}$$

The transition matrix $F_i(z)$ has two interesting properties. Defining the complex conjugate matrix $\tilde{F}_i(z) = F_i(z^{-1})$, we have:

$$\begin{aligned}\bar{F}_i(z)^T J_3 F_i(z) &= \frac{1-\rho_i}{1+\rho_i} J_3 = \frac{\eta_{i-1}}{\eta_i} J_3 \\ \bar{F}_i(z) &= J_1 F_i(z) J_1\end{aligned} \tag{6.6.7}$$

where J_1, J_3 are the 2×2 matrices:[†]

$$J_1 = \begin{bmatrix} 0 & 1 \\ 1 & 0 \end{bmatrix}, \quad J_3 = \begin{bmatrix} 1 & 0 \\ 0 & -1 \end{bmatrix} \tag{6.6.8}$$

In proving Eq. (6.6.7), we used the result $(1-\rho_i^2)/\tau_i^2 = (1-\rho_i)/(1+\rho_i) = \eta_{i-1}/\eta_i = n_i/n_{i-1}$. The first of Eqs. (6.6.7) implies *energy conservation*, that is, the energy flux into medium i is equal to the energy flux into medium $i+1$, or,

$$\frac{1}{2\eta_{i-1}}(\bar{E}_{i+}E_{i+} - \bar{E}_{i-}E_{i-}) = \frac{1}{2\eta_i}(\bar{E}_{i+1,+}E_{i+1,+} - \bar{E}_{i+1,-}E_{i+1,-}) \tag{6.6.9}$$

This can be expressed compactly in the form:

$$\bar{\mathbf{E}}_i^T J_3 \mathbf{E}_i = \frac{\eta_{i-1}}{\eta_i} \bar{\mathbf{E}}_{i+1}^T J_3 \mathbf{E}_{i+1}$$

which follows from Eq. (6.6.7):

$$\bar{\mathbf{E}}_i^T J_3 \mathbf{E}_i = \bar{\mathbf{E}}_{i+1}^T \bar{F}_i^T J_3 F_i \mathbf{E}_{i+1} = \frac{\eta_{i-1}}{\eta_i} \bar{\mathbf{E}}_{i+1}^T J_3 \mathbf{E}_{i+1}$$

The second of Eqs. (6.6.7) expresses *time-reversal invariance* and allows the construction of a second, linearly independent, solution of the recursions (6.6.5):

$$\hat{\mathbf{E}}_i = J_1 \bar{\mathbf{E}}_i = \begin{bmatrix} \bar{E}_{i-} \\ \bar{E}_{i+} \end{bmatrix} = J_1 \bar{F}_i(z) \bar{\mathbf{E}}_{i+1} = F_i(z) J_1 \bar{\mathbf{E}}_{i+1} = F_i(z) \hat{\mathbf{E}}_{i+1}$$

The recursions (6.6.5) may be iterated now to the rightmost interface. By an additional boundary match, we may pass to the right of interface $M+1$:

$$\mathbf{E}_i = F_i(z) F_{i+1}(z) \cdots F_M(z) F_{M+1} \mathbf{E}'_{M+1}$$

where we defined the last transition matrix as

$$F_{M+1} = \frac{1}{\tau_{M+1}} \begin{bmatrix} 1 & \rho_{M+1} \\ \rho_{M+1} & 1 \end{bmatrix} \tag{6.6.10}$$

More explicitly, we have:

$$\begin{bmatrix} E_{i+} \\ E_{i-} \end{bmatrix} = \frac{z^{(M+1-i)/2}}{\nu_i} \begin{bmatrix} 1 & \rho_i z^{-1} \\ \rho_i & z^{-1} \end{bmatrix} \begin{bmatrix} 1 & \rho_{i+1} z^{-1} \\ \rho_{i+1} & z^{-1} \end{bmatrix} \cdots \cdots \begin{bmatrix} 1 & \rho_M z^{-1} \\ \rho_M & z^{-1} \end{bmatrix} \begin{bmatrix} 1 & \rho_{M+1} \\ \rho_{M+1} & 1 \end{bmatrix} \begin{bmatrix} E'_{M+1,+} \\ E'_{M+1,-} \end{bmatrix} \tag{6.6.11}$$

[†]They are recognized as two of the three Pauli spin matrices.

where we defined $\nu_i = \tau_i \tau_{i+1} \cdots \tau_M \tau_{M+1}$. We introduce the following definition for the product of these matrices:

$$\begin{bmatrix} A_i(z) & C_i(z) \\ B_i(z) & D_i(z) \end{bmatrix} = \begin{bmatrix} 1 & \rho_i z^{-1} \\ \rho_i & z^{-1} \end{bmatrix} \cdots \begin{bmatrix} 1 & \rho_M z^{-1} \\ \rho_M & z^{-1} \end{bmatrix} \begin{bmatrix} 1 & \rho_{M+1} \\ \rho_{M+1} & 1 \end{bmatrix} \tag{6.6.12}$$

Because there are $M+1-i$ matrix factors that are first-order in z^{-1}, the quantities $A_i(z)$, $B_i(z)$, $C_i(z)$, and $D_i(z)$ will be *polynomials* of order $M+1-i$ in the variable z^{-1}. We may also express (6.6.12) in terms of the transition matrices $F_i(z)$:

$$\begin{bmatrix} A_i(z) & C_i(z) \\ B_i(z) & D_i(z) \end{bmatrix} = z^{-(M+1-i)/2} \nu_i F_i(z) \cdots F_M(z) F_{M+1} \tag{6.6.13}$$

It follows from Eq. (6.6.7) that (6.6.13) will also satisfy similar properties. Indeed, it can be shown easily that:

$$\begin{aligned}\bar{G}_i(z)^T J_3 G_i(z) &= \sigma_i^2 J_3, \qquad \text{where} \quad \sigma_i^2 = \prod_{m=i}^{M+1} (1-\rho_m^2) \\ G_i^R(z) &= J_1 G_i(z) J_1\end{aligned} \tag{6.6.14}$$

where $G_i(z)$ and its reverse $G_i^R(z)$ consisting of the *reversed* polynomials are:

$$G_i(z) = \begin{bmatrix} A_i(z) & C_i(z) \\ B_i(z) & D_i(z) \end{bmatrix}, \quad G_i^R(z) = \begin{bmatrix} A_i^R(z) & C_i^R(z) \\ B_i^R(z) & D_i^R(z) \end{bmatrix} \tag{6.6.15}$$

The reverse of a polynomial is obtained by reversing its coefficients, for example, if $A(z)$ has coefficient vector $\mathbf{a} = [a_0, a_1, a_2, a_3]$, then $A^R(z)$ will have coefficient vector $\mathbf{a}^R = [a_3, a_2, a_1, a_0]$. The reverse of a polynomial can be obtained directly in the z-domain by the property:

$$A^R(z) = z^{-d} A(z^{-1}) = z^{-d} \bar{A}(z)$$

where d is the degree of the polynomial. For example, we have:

$$\begin{aligned} A(z) &= a_0 + a_1 z^{-1} + a_2 z^{-2} + a_3 z^{-3} \\ A^R(z) &= a_3 + a_2 z^{-1} + a_1 z^{-2} + a_0 z^{-3} = z^{-3}(a_0 + a_1 z + a_2 z^2 + a_3 z^3) = z^{-3} \bar{A}(z) \end{aligned}$$

Writing the second of Eqs. (6.6.14) explicitly, we have:

$$\begin{bmatrix} A_i^R(z) & C_i^R(z) \\ B_i^R(z) & D_i^R(z) \end{bmatrix} = \begin{bmatrix} 0 & 1 \\ 1 & 0 \end{bmatrix} \begin{bmatrix} A_i(z) & C_i(z) \\ B_i(z) & D_i(z) \end{bmatrix} \begin{bmatrix} 0 & 1 \\ 1 & 0 \end{bmatrix} = \begin{bmatrix} D_i(z) & B_i(z) \\ C_i(z) & A_i(z) \end{bmatrix}$$

This implies that the polynomials $C_i(z), D_i(z)$ are the reverse of $B_i(z), A_i(z)$, that is, $C_i(z) = B_i^R(z), D_i(z) = A_i^R(z)$. Using this result, the first of Eqs. (6.6.14) implies the following constraint between $A_i(z)$ and $B_i(z)$:

$$\boxed{\bar{A}_i(z) A_i(z) - \bar{B}_i(z) B_i(z) = \sigma_i^2} \tag{6.6.16}$$

Thus, the product of matrices in Eq. (6.6.12) has the form:

$$\begin{bmatrix} A_i(z) & B_i^R(z) \\ B_i(z) & A_i^R(z) \end{bmatrix} = \begin{bmatrix} 1 & \rho_i z^{-1} \\ \rho_i & z^{-1} \end{bmatrix} \cdots \begin{bmatrix} 1 & \rho_M z^{-1} \\ \rho_M & z^{-1} \end{bmatrix} \begin{bmatrix} 1 & \rho_{M+1} \\ \rho_{M+1} & 1 \end{bmatrix} \tag{6.6.17}$$

This definition implies also the recursion:

$$\begin{bmatrix} A_i(z) & B_i^R(z) \\ B_i(z) & A_i^R(z) \end{bmatrix} = \begin{bmatrix} 1 & \rho_i z^{-1} \\ \rho_i & z^{-1} \end{bmatrix} \begin{bmatrix} A_{i+1}(z) & B_{i+1}^R(z) \\ B_{i+1}(z) & A_{i+1}^R(z) \end{bmatrix} \tag{6.6.18}$$

Therefore, each column will satisfy the same recursion:[†]

$$\begin{bmatrix} A_i(z) \\ B_i(z) \end{bmatrix} = \begin{bmatrix} 1 & \rho_i z^{-1} \\ \rho_i & z^{-1} \end{bmatrix} \begin{bmatrix} A_{i+1}(z) \\ B_{i+1}(z) \end{bmatrix} \quad \text{(forward recursion)} \tag{6.6.19}$$

for $i = M, M-1, \ldots, 1$, and initialized by the 0th degree polynomials:

$$\begin{bmatrix} A_{M+1}(z) \\ B_{M+1}(z) \end{bmatrix} = \begin{bmatrix} 1 \\ \rho_{M+1} \end{bmatrix} \tag{6.6.20}$$

Eq. (6.6.11) reads now:

$$\begin{bmatrix} E_{i+} \\ E_{i-} \end{bmatrix} = \frac{z^{(M+1-i)/2}}{\nu_i} \begin{bmatrix} A_i(z) & B_i^R(z) \\ B_i(z) & A_i^R(z) \end{bmatrix} \begin{bmatrix} E'_{M+1,+} \\ E'_{M+1,-} \end{bmatrix} \tag{6.6.21}$$

Setting $i = 1$, we find the relationship between the fields incident on the dielectric structure from the left to those incident from the right:

$$\begin{bmatrix} E_{1+} \\ E_{1-} \end{bmatrix} = \frac{z^{M/2}}{\nu_1} \begin{bmatrix} A_1(z) & B_1^R(z) \\ B_1(z) & A_1^R(z) \end{bmatrix} \begin{bmatrix} E'_{M+1,+} \\ E'_{M+1,-} \end{bmatrix} \tag{6.6.22}$$

where $\nu_1 = \tau_1 \tau_2 \cdots \tau_{M+1}$. The polynomials $A_1(z)$ and $B_1(z)$ have degree M and are obtained by the recursion (6.6.19). These polynomials incorporate all the multiple reflections and reverberatory effects of the structure.

In referring to the overall transition matrix of the structure, we may drop the subscripts 1 and $M+1$ and write Eq. (6.6.22) in the more convenient form:

$$\begin{bmatrix} E_+ \\ E_- \end{bmatrix} = \frac{z^{M/2}}{\nu} \begin{bmatrix} A(z) & B^R(z) \\ B(z) & A^R(z) \end{bmatrix} \begin{bmatrix} E'_+ \\ E'_- \end{bmatrix} \quad \text{(transfer matrix)} \tag{6.6.23}$$

Fig. 6.6.2 shows the general case of left- and right-incident fields, as well as when the fields are incident only from the left or only from the right.

For both the left- and right-incident cases, the corresponding reflection and transmission responses $\Gamma, \mathcal{T}$ and $\Gamma', \mathcal{T}'$ will satisfy Eq. (6.6.23):

$$\begin{aligned} \begin{bmatrix} 1 \\ \Gamma \end{bmatrix} &= \frac{z^{M/2}}{\nu} \begin{bmatrix} A(z) & B^R(z) \\ B(z) & A^R(z) \end{bmatrix} \begin{bmatrix} \mathcal{T} \\ 0 \end{bmatrix} \\ \begin{bmatrix} 0 \\ \mathcal{T}' \end{bmatrix} &= \frac{z^{M/2}}{\nu} \begin{bmatrix} A(z) & B^R(z) \\ B(z) & A^R(z) \end{bmatrix} \begin{bmatrix} \Gamma' \\ 1 \end{bmatrix} \end{aligned} \tag{6.6.24}$$

[†]Forward means order-increasing: as the index i decreases, the polynomial order $M+1-i$ increases.

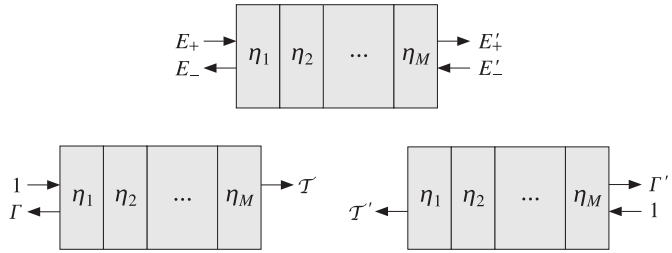

Fig. 6.6.2 Reflection and transmission responses of a multilayer structure.

Solving for $\Gamma, \mathcal{T}$, we find:

$$\boxed{\Gamma(z) = \frac{B(z)}{A(z)}, \quad \mathcal{T}(z) = \frac{\nu z^{-M/2}}{A(z)}} \tag{6.6.25}$$

Similarly, we find for $\Gamma', \mathcal{T}'$:

$$\boxed{\Gamma'(z) = -\frac{B^R(z)}{A(z)}, \quad \mathcal{T}'(z) = \frac{\nu' z^{-M/2}}{A(z)}} \tag{6.6.26}$$

where the constants ν and ν' are the products of the left and right transmission coefficients $\tau_i = 1 + \rho_i$ and $\tau'_i = 1 - \rho_i$, that is,

$$\nu = \prod_{i=1}^{M+1} \tau_i = \prod_{i=1}^{M+1} (1 + \rho_i), \quad \nu' = \prod_{i=1}^{M+1} \tau'_i = \prod_{i=1}^{M+1} (1 - \rho_i) \tag{6.6.27}$$

In deriving the expression for $\mathcal{T}'$, we used the result (6.6.16), which for $i = 1$ reads:

$$\bar{A}(z) A(z) - \bar{B}(z) B(z) = \sigma^2, \qquad \text{where} \quad \sigma^2 = \prod_{i=1}^{M+1} (1 - \rho_i^2) \tag{6.6.28}$$

Because $A^R(z) = z^{-M} \bar{A}(z)$, we can rewrite (6.6.28) in the form:

$$A(z) A^R(z) - B(z) B^R(z) = \sigma^2 z^{-M} \tag{6.6.29}$$

Noting that $\nu\nu' = \sigma^2$ and that

$$\frac{\nu'}{\nu} = \prod_{i=1}^{M+1} \frac{1 - \rho_i}{1 + \rho_i} = \prod_{i=1}^{M+1} \frac{\eta_{i-1}}{\eta_i} = \frac{\eta_a}{\eta_b},$$

we may replace ν and ν' by the more convenient forms:

$$\nu = \sigma \sqrt{\frac{\eta_b}{\eta_a}}, \quad \nu' = \sigma \sqrt{\frac{\eta_a}{\eta_b}} \tag{6.6.30}$$

Then, the transmission responses $\mathcal{T}$ and $\mathcal{T}'$ can be expressed as:

$$\boxed{\mathcal{T}(z)=\sqrt{\frac{\eta_b}{\eta_a}}\,T(z),\quad \mathcal{T}'(z)=\sqrt{\frac{\eta_a}{\eta_b}}\,T(z),\quad T(z)=\frac{\sigma z^{-M/2}}{A(z)}} \tag{6.6.31}$$

The magnitude squared of $T(z)$ represents the transmittance, that is, the ratio of the transmitted to incident powers, whereas $\mathcal{T}$ is the corresponding ratio of the electric fields. Indeed, assuming $E'_- = 0$, we have $\mathcal{T} = E'_+/E_+$ and find:

$$\frac{\mathcal{P}_{\text{transmitted}}}{\mathcal{P}_{\text{incident}}}=\frac{\frac{1}{2\eta_b}|E'_+|^2}{\frac{1}{2\eta_a}|E_+|^2}=\frac{\eta_a}{\eta_b}|\mathcal{T}|^2=|T|^2 \tag{6.6.32}$$

where we used Eq. (6.6.31). Similarly, if the incident fields are from the right, then assuming $E_+ = 0$, the corresponding transmission coefficient will be $\mathcal{T}' = E_-/E'_-$, and we find for the left-going transmittance:

$$\frac{\mathcal{P}'_{\text{transmitted}}}{\mathcal{P}'_{\text{incident}}}=\frac{\frac{1}{2\eta_a}|E_-|^2}{\frac{1}{2\eta_b}|E'_-|^2}=\frac{\eta_b}{\eta_a}|\mathcal{T}'|^2=|T|^2 \tag{6.6.33}$$

Eqs. (6.6.32) and (6.6.33) state that the transmittance is the *same* from either side of the structure. This result remains valid even when the slabs are lossy.

The *frequency response* of the structure is obtained by setting $z = e^{j\omega T_s}$. Denoting $A(e^{j\omega T_s})$ simply by $A(\omega)$, we may express Eq. (6.6.28) in the form:

$$|A(\omega)|^2-|B(\omega)|^2=\sigma^2 \tag{6.6.34}$$

This implies the following relationship between reflectance and transmittance:

$$\boxed{|\Gamma(\omega)|^2+|T(\omega)|^2=1} \tag{6.6.35}$$

Indeed, dividing Eq. (6.6.34) by $|A(\omega)|^2$ and using Eq. (6.6.31), we have:

$$1-\left|\frac{B(\omega)}{A(\omega)}\right|^2=\frac{\sigma^2}{|A(\omega)|^2}=\left|\frac{\sigma e^{-jM\omega T_s/2}}{A(\omega)}\right|^2 \quad\Rightarrow\quad 1-|\Gamma(\omega)|^2=|T(\omega)|^2$$

Scattering Matrix

The transfer matrix in Eq. (6.6.23) relates the incident and reflected fields at the left of the structure to those at the right of the structure. Using Eqs. (6.6.25), (6.6.26), and (6.6.29), we may rearrange the transfer matrix (6.6.23) into a *scattering matrix* form that relates the *incoming* fields E_+, E'_- to the *outgoing* fields E_-, E'_+. We have:

$$\begin{bmatrix} E_- \\ E'_+ \end{bmatrix}=\begin{bmatrix} \Gamma(z) & \mathcal{T}'(z) \\ \mathcal{T}(z) & \Gamma'(z) \end{bmatrix}\begin{bmatrix} E_+ \\ E'_- \end{bmatrix} \qquad \text{(scattering matrix)} \tag{6.6.36}$$

The elements of the scattering matrix are referred to as the *S-parameters* and are used widely in the characterization of two-port (and multi-port) networks at microwave frequencies.

We discuss S-parameters in Sec. 14.1. It is a common convention in the literature to normalize the fields to the impedances of the left and right media (the generator and load impedances), as follows:

$$\mathcal{E}_\pm=\frac{1}{\sqrt{\eta_a}}E_\pm=\frac{E\pm\eta_a H}{2\sqrt{\eta_a}},\qquad \mathcal{E}'_\pm=\frac{1}{\sqrt{\eta_b}}E'_\pm=\frac{E'\pm\eta_b H'}{2\sqrt{\eta_b}} \tag{6.6.37}$$

Such normalized fields are referred to as *power waves* [1139]. Using the results of Eq. (6.6.31), the scattering matrix may be written in terms of the normalized fields in the more convenient form:

$$\begin{bmatrix} \mathcal{E}_- \\ \mathcal{E}'_+ \end{bmatrix}=\begin{bmatrix} \Gamma(z) & T(z) \\ T(z) & \Gamma'(z) \end{bmatrix}\begin{bmatrix} \mathcal{E}_+ \\ \mathcal{E}'_- \end{bmatrix}=S(z)\begin{bmatrix} \mathcal{E}_+ \\ \mathcal{E}'_- \end{bmatrix} \tag{6.6.38}$$

so that $S(z)$ is now a symmetric matrix:

$$S(z)=\begin{bmatrix} \Gamma(z) & T(z) \\ T(z) & \Gamma'(z) \end{bmatrix}\qquad \text{(scattering matrix)} \tag{6.6.39}$$

One can verify also that Eqs. (6.6.25), (6.6.26), and (6.6.28) imply the following unitarity properties of $S(z)$:

$$\bar{S}(z)^T S(z)=I,\qquad S(\omega)^\dagger S(\omega)=I,\qquad \text{(unitarity)} \tag{6.6.40}$$

where I is the 2×2 identity matrix, $\bar{S}(z)=S(z^{-1})$, and $S(\omega)$ denotes $S(z)$ with $z = e^{j\omega T_s}$, so that $\bar{S}(\omega)^T$ becomes the hermitian conjugate $S(\omega)^\dagger = S(\omega)^{*T}$.

The unitarity condition is equivalent to the power conservation condition that the net incoming power into the (lossless) multilayer structure is equal to the net outgoing reflected power from the structure. Indeed, in terms of the power waves, we have:

$$\begin{aligned}\mathcal{P}_{\text{out}}&=\frac{1}{2\eta_a}|E_-|^2+\frac{1}{2\eta_b}|E'_+|^2=\frac{1}{2}|\mathcal{E}_-|^2+\frac{1}{2}|\mathcal{E}'_+|^2\\&=\frac{1}{2}[\mathcal{E}_-^*,\mathcal{E}_+^{*\prime}]\begin{bmatrix} \mathcal{E}_- \\ \mathcal{E}'_+ \end{bmatrix}=\frac{1}{2}[\mathcal{E}_+^*,\mathcal{E}_-^{*\prime}]S^\dagger S\begin{bmatrix} \mathcal{E}_+ \\ \mathcal{E}'_- \end{bmatrix}=\frac{1}{2}[\mathcal{E}_+^*,\mathcal{E}_-^{*\prime}]I\begin{bmatrix} \mathcal{E}_+ \\ \mathcal{E}'_- \end{bmatrix}\\&=\frac{1}{2}|\mathcal{E}_+|^2+\frac{1}{2}|\mathcal{E}'_-|^2=\frac{1}{2\eta_a}|E_+|^2+\frac{1}{2\eta_b}|E'_-|^2=\mathcal{P}_{\text{in}}\end{aligned}$$

Layer Recursions

Next, we discuss the layer recursions. The reflection responses at the successive interfaces of the structure are given by similar equations to (6.6.25). We have $\Gamma_i(z) = B_i(z)/A_i(z)$ at the ith interface and $\Gamma_{i+1}(z) = B_{i+1}(z)/A_{i+1}(z)$ at the next one. Using Eq. (6.6.19), we find that the responses Γ_i satisfy the following recursion, which is equivalent to Eq. (6.1.3):

$$\boxed{\Gamma_i(z)=\frac{\rho_i+z^{-1}\Gamma_{i+1}(z)}{1+\rho_i z^{-1}\Gamma_{i+1}(z)}},\quad i=M,M-1,\dots,1 \tag{6.6.41}$$

It starts at $\Gamma_{M+1}(z) = \rho_{M+1}$ and ends with $\Gamma(z) = \Gamma_1(z)$. The impedances at the interfaces satisfy Eq. (6.1.5), which takes the specialized form in the case of equal phase thicknesses:

$$\boxed{Z_i(s) = \eta_i \frac{Z_{i+1}(s) + \eta_i s}{\eta_i + s Z_{i+1}(s)}}, \quad i = M, M-1, \ldots, 1 \tag{6.6.42}$$

where we defined the variable s via the *bilinear transformation*:

$$s = \frac{1 - z^{-1}}{1 + z^{-1}} \tag{6.6.43}$$

Note that if $z = e^{2j\delta}$, then $s = j \tan\delta$. It is more convenient to think of the impedances $Z_i(s)$ as functions of the variable s and the reflection responses $\Gamma_i(z)$ as functions of the variable z.

To summarize, given the characteristic impedances $\{\eta_a, \eta_1, \ldots, \eta_M, \eta_b\}$, equivalently, the refractive indices $\{n_1, n_1, \ldots, n_M\}$ of a multilayered structure, we can compute the corresponding reflection coefficients $\{\rho_1, \rho_2, \ldots, \rho_{M+1}\}$ and then carry out the polynomial recursions (6.6.19), eventually arriving at the final Mth order polynomials $A(z)$ and $B(z)$, which define via Eq. (6.6.25) the overall reflection and transmission responses of the structure.

Conversely, given the final polynomials $A_1(z) = A(z)$ and $B_1(z) = B(z)$, we invert the recursion (6.6.19) and "peel off" one layer at a time, until we arrive at the rightmost interface. In the process, we extract the reflection coefficients $\{\rho_1, \rho_2, \ldots, \rho_{M+1}\}$, as well as the characteristic impedances and refractive indices of the structure.

This inverse recursion is based on the property that the reflection coefficients appear in the first and last coefficients of the polynomials $B_i(z)$ and $A_i(z)$. Indeed, if we define these coefficients by the expansions:

$$B_i(z) = \sum_{m=0}^{M+1-i} b_i(m) z^{-m}, \quad A_i(z) = \sum_{m=0}^{M+1-i} a_i(m) z^{-m}$$

then, it follows from Eq. (6.6.19) that the first coefficients are:

$$b_i(0) = \rho_i, \quad a_i(0) = 1 \tag{6.6.44}$$

whereas the last coefficients are:

$$b_i(M+1-i) = \rho_{M+1}, \quad a_i(M+1-i) = \rho_{M+1}\rho_i \tag{6.6.45}$$

Inverting the transition matrix in Eq. (6.6.19), we obtain the backward recursion:[†]

$$\begin{bmatrix} A_{i+1}(z) \\ B_{i+1}(z) \end{bmatrix} = \frac{1}{1-\rho_i^2} \begin{bmatrix} 1 & -\rho_i \\ -\rho_i z & z \end{bmatrix} \begin{bmatrix} A_i(z) \\ B_i(z) \end{bmatrix} \quad \text{(backward recursion)} \tag{6.6.46}$$

[†]Backward means order-decreasing: as the index i increases, the polynomial order $M+1-i$ decreases.

for $i = 1, 2, \ldots, M$, where $\rho_i = b_i(0)$. This recursion starts with the knowledge of $A_1(z)$ and $B_1(z)$. We note that each step of the recursion reduces the order of the polynomials by one, until we reach the 0th order polynomials $A_{M+1}(z) = 1$ and $B_{M+1}(z) = \rho_{M+1}$.

The reverse recursions can also be applied directly to the reflection responses $\Gamma_i(z)$ and wave impedances $Z_i(s)$. It follows from Eq. (6.6.41) that the reflection coefficient ρ_i can be extracted from $\Gamma_i(z)$ if we set $z = \infty$, that is, $\rho_i = \Gamma_i(\infty)$. Then, solving Eq. (6.1.3) for $\Gamma_{i+1}(z)$, we obtain:

$$\boxed{\Gamma_{i+1}(z) = z \frac{\Gamma_i(z) - \rho_i}{1 - \rho_i \Gamma_i(z)}}, \quad i = 1, 2, \ldots, M \tag{6.6.47}$$

Similarly, it follows from Eq. (6.6.42) that the characteristic impedance η_i can be extracted from $Z_i(s)$ by setting $s = 1$, which is equivalent to $z = \infty$ under the transformation (6.6.43). Thus, $\eta_i = Z_i(1)$ and the inverse of (6.6.42) becomes:

$$\boxed{Z_{i+1}(s) = \eta_i \frac{Z_i(s) - s\eta_i}{\eta_i - s Z_i(s)}}, \quad i = 1, 2, \ldots, M \tag{6.6.48}$$

The necessary and sufficient condition that the extracted reflection coefficients ρ_i and the media impedances η_i are realizable, that is, $|\rho_i| < 1$ or $\eta_i > 0$, is that the starting polynomial $A(z)$ be a *minimum-phase polynomial* in z^{-1}, that is, it must have all its zeros inside the unit circle on the z-plane. This condition is in turn equivalent to the requirement that the transmission and reflection responses $T(z)$ and $\Gamma(z)$ be *stable and causal* transfer functions.

The order-increasing and order-decreasing recursions Eqs. (6.6.19) and (6.6.46) can also be expressed in terms of the vectors of coefficients of the polynomials $A_i(z)$ and $B_i(z)$. Defining the column vectors:

$$\mathbf{a}_i = \begin{bmatrix} a_i(0) \\ a_i(1) \\ \vdots \\ a_i(M+1-i) \end{bmatrix}, \qquad \mathbf{b}_i = \begin{bmatrix} b_i(0) \\ b_i(1) \\ \vdots \\ b_i(M+1-i) \end{bmatrix}$$

we obtain for Eq. (6.6.19), with $i = M, M-1, \ldots, 1$:

$$\begin{aligned} \mathbf{a}_i &= \begin{bmatrix} \mathbf{a}_{i+1} \\ 0 \end{bmatrix} + \rho_i \begin{bmatrix} 0 \\ \mathbf{b}_{i+1} \end{bmatrix} \\ \mathbf{b}_i &= \rho_i \begin{bmatrix} \mathbf{a}_{i+1} \\ 0 \end{bmatrix} + \begin{bmatrix} 0 \\ \mathbf{b}_{i+1} \end{bmatrix} \end{aligned} \quad \text{(forward recursion)} \tag{6.6.49}$$

and initialized at $\mathbf{a}_{M+1} = [1]$ and $\mathbf{b}_{M+1} = [\rho_{M+1}]$. Similarly, the backward recursions (6.6.46) are initialized at the Mth order polynomials $\mathbf{a}_1 = \mathbf{a}$ and $\mathbf{b}_1 = \mathbf{b}$. For $i = 1, 2, \ldots, M$ and $\rho_i = b_i(0)$, we have:

$$\begin{bmatrix} \mathbf{a}_{i+1} \\ 0 \end{bmatrix} = \frac{\mathbf{a}_i - \rho_i \mathbf{b}_i}{1-\rho_i^2}$$
$$\begin{bmatrix} 0 \\ \mathbf{b}_{i+1} \end{bmatrix} = \frac{-\rho_i \mathbf{a}_i + \mathbf{b}_i}{1-\rho_i^2} \qquad \text{(backward recursion)} \tag{6.6.50}$$

Example 6.6.1: Determine the number of layers M, the reflection coefficients at the $M+1$ interfaces, and the refractive indices of the $M+2$ media for a multilayer structure whose overall reflection response is given by:

$$\Gamma(z) = \frac{B(z)}{A(z)} = \frac{-0.1 - 0.188z^{-1} - 0.35z^{-2} + 0.5z^{-3}}{1 - 0.1z^{-1} - 0.064z^{-2} - 0.05z^{-3}}$$

Solution: From the degree of the polynomials, the number of layers is $M = 3$. The starting polynomials in the backward recursion (6.6.50) are:

$$\mathbf{a}_1 = \mathbf{a} = \begin{bmatrix} 1.000 \\ -0.100 \\ -0.064 \\ -0.050 \end{bmatrix}, \quad \mathbf{b}_1 = \mathbf{b} = \begin{bmatrix} -0.100 \\ -0.188 \\ -0.350 \\ 0.500 \end{bmatrix}$$

From the first and last coefficients of $\mathbf{b}_1$, we find $\rho_1 = -0.1$ and $\rho_4 = 0.5$. Setting $i = 1$, the first step of the recursion gives:

$$\begin{bmatrix} \mathbf{a}_2 \\ 0 \end{bmatrix} = \frac{\mathbf{a}_1 - \rho_1 \mathbf{b}_1}{1-\rho_1^2} = \begin{bmatrix} 1.000 \\ -0.120 \\ -0.100 \\ 0.000 \end{bmatrix}, \quad \begin{bmatrix} 0 \\ \mathbf{b}_2 \end{bmatrix} = \frac{-\rho_1 \mathbf{a}_1 + \mathbf{b}_1}{1-\rho_1^2} = \begin{bmatrix} 0.000 \\ -0.200 \\ -0.360 \\ 0.500 \end{bmatrix}$$

Thus,

$$\mathbf{a}_2 = \begin{bmatrix} 1.000 \\ -0.120 \\ -0.100 \end{bmatrix}, \quad \mathbf{b}_2 = \begin{bmatrix} -0.200 \\ -0.360 \\ 0.500 \end{bmatrix}$$

The first coefficient of $\mathbf{b}_2$ is $\rho_2 = -0.2$ and the next step of the recursion gives:

$$\begin{bmatrix} \mathbf{a}_3 \\ 0 \end{bmatrix} = \frac{\mathbf{a}_2 - \rho_2 \mathbf{b}_2}{1-\rho_2^2} = \begin{bmatrix} 1.0 \\ -0.2 \\ 0.0 \end{bmatrix}, \quad \begin{bmatrix} 0 \\ \mathbf{b}_3 \end{bmatrix} = \frac{-\rho_2 \mathbf{a}_2 + \mathbf{b}_2}{1-\rho_2^2} = \begin{bmatrix} 0.0 \\ -0.4 \\ 0.5 \end{bmatrix}$$

Thus,

$$\mathbf{a}_3 = \begin{bmatrix} 1.0 \\ -0.2 \end{bmatrix}, \quad \mathbf{b}_3 = \begin{bmatrix} -0.4 \\ 0.5 \end{bmatrix} \quad \Rightarrow \quad \rho_3 = -0.4$$

The last step of the recursion for $i = 3$ is not necessary because we have already determined $\rho_4 = 0.5$. Thus, the four reflection coefficients are:

$$[\rho_1, \rho_2, \rho_3, \rho_4] = [-0.1, -0.2, -0.4, 0.5]$$

The corresponding refractive indices can be obtained by solving Eq. (6.1.1), that is, $n_i = n_{i-1}(1-\rho_i)/(1+\rho_i)$. Starting with $i = 1$ and $n_0 = n_a = 1$, we obtain:

$$[n_a, n_1, n_2, n_3, n_b] = [1, 1.22, 1.83, 4.28, 1.43]$$

The same results can be obtained by working with the polynomial version of the recursion, Eq. (6.6.46). □

Example 6.6.2: Consider the quarter-quarter antireflection coating shown in Fig. 6.2.2 with refractive indices $[n_a, n_1, n_2, n_b] = [1, 1.38, 1.63, 1.50]$. Determine the reflection coefficients at the three interfaces and the overall reflection response $\Gamma(z)$ of the structure.

Solution: In this problem we carry out the forward layer recursion starting from the rightmost layer. The reflection coefficients computed from Eq. (6.1.1) are:

$$[\rho_1, \rho_2, \rho_3] = [-0.1597, -0.0831, 0.0415]$$

Starting the forward recursion with $\mathbf{a}_3 = [1]$ and $\mathbf{b}_3 = [\rho_3] = [0.0415]$, we build the first order polynomials:

$$\mathbf{a}_2 = \begin{bmatrix} \mathbf{a}_3 \\ 0 \end{bmatrix} + \rho_2 \begin{bmatrix} 0 \\ \mathbf{b}_3 \end{bmatrix} = \begin{bmatrix} 1.0000 \\ 0.0000 \end{bmatrix} + (-0.0831) \begin{bmatrix} 0.0000 \\ 0.0415 \end{bmatrix} = \begin{bmatrix} 1.0000 \\ -0.0034 \end{bmatrix}$$
$$\mathbf{b}_2 = \rho_2 \begin{bmatrix} \mathbf{a}_3 \\ 0 \end{bmatrix} + \begin{bmatrix} 0 \\ \mathbf{b}_3 \end{bmatrix} = (-0.0831) \begin{bmatrix} 1.0000 \\ 0.0000 \end{bmatrix} + \begin{bmatrix} 0.0000 \\ 0.0415 \end{bmatrix} = \begin{bmatrix} -0.0831 \\ 0.0415 \end{bmatrix}$$

Then, we build the 2nd order polynomials at the first interface:

$$\mathbf{a}_1 = \begin{bmatrix} \mathbf{a}_2 \\ 0 \end{bmatrix} + \rho_1 \begin{bmatrix} 0 \\ \mathbf{b}_2 \end{bmatrix} = \begin{bmatrix} 1.0000 \\ 0.0098 \\ -0.0066 \end{bmatrix}, \quad \mathbf{b}_1 = \rho_1 \begin{bmatrix} \mathbf{a}_2 \\ 0 \end{bmatrix} + \begin{bmatrix} 0 \\ \mathbf{b}_2 \end{bmatrix} = \begin{bmatrix} -0.1597 \\ -0.0825 \\ 0.0415 \end{bmatrix}$$

Thus, the overall reflection response is:

$$\Gamma(z) = \Gamma_1(z) = \frac{B_1(z)}{A_1(z)} = \frac{-0.1597 - 0.0825z^{-1} + 0.0415z^{-2}}{1 + 0.0098z^{-1} - 0.0066z^{-2}}$$

Applying the reverse recursion on this reflection response would generate the same reflection coefficients ρ_1, ρ_2, ρ_3. □

Example 6.6.3: Determine the overall reflection response of the quarter-half-quarter coating of Fig. 6.2.2 by thinking of the half-wavelength layer as two quarter-wavelength layers of the same refractive index.

Solution: There are $M = 4$ quarter-wave layers with refractive indices:

$$[n_a, n_1, n_2, n_3, n_4, n_b] = [1, 1.38, 2.20, 2.20, 1.63, 1.50]$$

The corresponding reflection coefficients are:

$$[\rho_1, \rho_2, \rho_3, \rho_4, \rho_5] = [-0.1597, -0.2291, 0, 0.1488, 0.0415]$$

where the reflection coefficient at the imaginary interface separating the two halves of the half-wave layer is zero. Starting the forward recursion with $\mathbf{a}_5 = [1]$, $\mathbf{b}_5 = [\rho_5] = [0.0415]$, we compute the higher-order polynomials:

$$\mathbf{a}_4 = \begin{bmatrix} \mathbf{a}_5 \\ 0 \end{bmatrix} + \rho_4 \begin{bmatrix} 0 \\ \mathbf{b}_5 \end{bmatrix} = \begin{bmatrix} 1.0000 \\ 0.0062 \end{bmatrix}, \quad \mathbf{b}_4 = \rho_4 \begin{bmatrix} \mathbf{a}_5 \\ 0 \end{bmatrix} + \begin{bmatrix} 0 \\ \mathbf{b}_5 \end{bmatrix} = \begin{bmatrix} 0.1488 \\ 0.0415 \end{bmatrix}$$

$$\mathbf{a}_3 = \begin{bmatrix} \mathbf{a}_4 \\ 0 \end{bmatrix} + \rho_3 \begin{bmatrix} 0 \\ \mathbf{b}_4 \end{bmatrix} = \begin{bmatrix} 1.0000 \\ 0.0062 \\ 0.0000 \end{bmatrix}, \quad \mathbf{b}_3 = \rho_3 \begin{bmatrix} \mathbf{a}_4 \\ 0 \end{bmatrix} + \begin{bmatrix} 0 \\ \mathbf{b}_4 \end{bmatrix} = \begin{bmatrix} 0.0000 \\ 0.1488 \\ 0.0415 \end{bmatrix}$$

$$\mathbf{a}_2 = \begin{bmatrix} \mathbf{a}_3 \\ 0 \end{bmatrix} + \rho_2 \begin{bmatrix} 0 \\ \mathbf{b}_3 \end{bmatrix} = \begin{bmatrix} 1.0000 \\ 0.0062 \\ -0.0341 \\ -0.0095 \end{bmatrix}, \quad \mathbf{b}_2 = \rho_2 \begin{bmatrix} \mathbf{a}_3 \\ 0 \end{bmatrix} + \begin{bmatrix} 0 \\ \mathbf{b}_3 \end{bmatrix} = \begin{bmatrix} -0.2291 \\ -0.0014 \\ 0.1488 \\ 0.0415 \end{bmatrix}$$

$$\mathbf{a}_1 = \begin{bmatrix} \mathbf{a}_2 \\ 0 \end{bmatrix} + \rho_1 \begin{bmatrix} 0 \\ \mathbf{b}_2 \end{bmatrix} = \begin{bmatrix} 1.0000 \\ 0.0428 \\ -0.0339 \\ -0.0333 \\ -0.0066 \end{bmatrix}, \quad \mathbf{b}_1 = \rho_1 \begin{bmatrix} \mathbf{a}_2 \\ 0 \end{bmatrix} + \begin{bmatrix} 0 \\ \mathbf{b}_2 \end{bmatrix} = \begin{bmatrix} -0.1597 \\ -0.2300 \\ 0.0040 \\ 0.1503 \\ 0.0415 \end{bmatrix}$$

Thus, the reflection response will be:

$$\Gamma(z) = \frac{B_1(z)}{A_1(z)} = \frac{-0.1597 - 0.2300z^{-1} + 0.0040z^{-2} + 0.1502z^{-3} + 0.0415z^{-4}}{1 + 0.0428z^{-1} - 0.0339z^{-2} - 0.0333z^{-3} - 0.0066z^{-4}}$$

We note that because $\rho_3 = 0$, the polynomials $A_3(z)$ and $A_4(z)$ are the same and $B_3(z)$ is simply the delayed version of $B_4(z)$, that is, $B_3(z) = z^{-1}B_4(z)$. □

Example 6.6.4: Determine the reflection polynomials for the cases $M = 1$, $M = 2$, and $M = 3$ with reflection coefficients $\{\rho_1, \rho_2\}$, $\{\rho_1, \rho_2, \rho_3\}$, and $\{\rho_1, \rho_2, \rho_3, \rho_4\}$, respectively.

Solution: For $M = 1$, we have $A_2(z) = 1$ and $B_2(z) = \rho_2$. Then, Eq. (6.6.19) gives:

$$\begin{bmatrix} A_1(z) \\ B_1(z) \end{bmatrix} = \begin{bmatrix} 1 & \rho_1 z^{-1} \\ \rho_1 & z^{-1} \end{bmatrix} \begin{bmatrix} A_2(z) \\ B_2(z) \end{bmatrix} = \begin{bmatrix} 1 & \rho_1 z^{-1} \\ \rho_1 & z^{-1} \end{bmatrix} \begin{bmatrix} 1 \\ \rho_2 \end{bmatrix} = \begin{bmatrix} 1 + \rho_1\rho_2 z^{-1} \\ \rho_1 + \rho_2 z^{-1} \end{bmatrix}$$

For $M = 2$, we start with $A_3(z) = 1$ and $B_3(z) = \rho_3$. The first step of the recursion gives:

$$\begin{bmatrix} A_2(z) \\ B_2(z) \end{bmatrix} = \begin{bmatrix} 1 & \rho_2 z^{-1} \\ \rho_2 & z^{-1} \end{bmatrix} \begin{bmatrix} 1 \\ \rho_3 \end{bmatrix} = \begin{bmatrix} 1 + \rho_2\rho_3 z^{-1} \\ \rho_2 + \rho_3 z^{-1} \end{bmatrix}$$

and the second step:

$$\begin{bmatrix} A_1(z) \\ B_1(z) \end{bmatrix} = \begin{bmatrix} 1 & \rho_1 z^{-1} \\ \rho_1 & z^{-1} \end{bmatrix} \begin{bmatrix} 1 + \rho_2\rho_3 z^{-1} \\ \rho_2 + \rho_3 z^{-1} \end{bmatrix} = \begin{bmatrix} 1 + \rho_2(\rho_1 + \rho_3)z^{-1} + \rho_1\rho_3 z^{-2} \\ \rho_1 + \rho_2(1 + \rho_1\rho_3)z^{-1} + \rho_3 z^{-2} \end{bmatrix}$$

For $M = 3$, we have $A_4(z) = 1$ and $B_4(z) = \rho_4$. The first and second steps give:

$$\begin{bmatrix} A_3(z) \\ B_3(z) \end{bmatrix} = \begin{bmatrix} 1 & \rho_3 z^{-1} \\ \rho_3 & z^{-1} \end{bmatrix} \begin{bmatrix} 1 \\ \rho_4 \end{bmatrix} = \begin{bmatrix} 1 + \rho_3\rho_4 z^{-1} \\ \rho_3 + \rho_4 z^{-1} \end{bmatrix}$$

$$\begin{bmatrix} A_2(z) \\ B_2(z) \end{bmatrix} = \begin{bmatrix} 1 & \rho_2 z^{-1} \\ \rho_2 & z^{-1} \end{bmatrix} \begin{bmatrix} 1 + \rho_3\rho_4 z^{-1} \\ \rho_3 + \rho_4 z^{-1} \end{bmatrix} = \begin{bmatrix} 1 + \rho_3(\rho_2 + \rho_4)z^{-1} + \rho_2\rho_4 z^{-2} \\ \rho_2 + \rho_3(1 + \rho_2\rho_4)z^{-1} + \rho_4 z^{-2} \end{bmatrix}$$

Then, the final step gives:

$$\begin{bmatrix} A_1(z) \\ B_1(z) \end{bmatrix} = \begin{bmatrix} 1 & \rho_1 z^{-1} \\ \rho_1 & z^{-1} \end{bmatrix} \begin{bmatrix} 1 + \rho_3(\rho_2 + \rho_4)z^{-1} + \rho_2\rho_4 z^{-2} \\ \rho_2 + \rho_3(1 + \rho_2\rho_4)z^{-1} + \rho_4 z^{-2} \end{bmatrix}$$

$$= \begin{bmatrix} 1 + (\rho_1\rho_2 + \rho_2\rho_3 + \rho_3\rho_4)z^{-1} + (\rho_1\rho_3 + \rho_2\rho_4 + \rho_1\rho_2\rho_3\rho_4)z^{-2} + \rho_1\rho_4 z^{-3} \\ \rho_1 + (\rho_2 + \rho_1\rho_2\rho_3 + \rho_1\rho_3\rho_4)z^{-1} + (\rho_3 + \rho_1\rho_2\rho_4 + \rho_2\rho_3\rho_4)z^{-2} + \rho_4 z^{-3} \end{bmatrix}$$

As expected, in all cases the first and last coefficients of $A_i(z)$ are 1 and $\rho_i\rho_{M+1}$ and those of $B_i(z)$ are ρ_i and ρ_{M+1}.

An approximation that is often made in practice is to assume that the ρ_is are small and ignore all the terms that involve two or more factors of ρ_i. In this approximation, we have for the polynomials and the reflection response $\Gamma(z) = B_1(z)/A_1(z)$, for the $M = 3$ case:

$$\begin{aligned} &A_1(z) = 1 \\ &B_1(z) = \rho_1 + \rho_2 z^{-1} + \rho_3 z^{-2} + \rho_4 z^{-3} \end{aligned} \qquad \Rightarrow \quad \Gamma(z) = \rho_1 + \rho_2 z^{-1} + \rho_3 z^{-2} + \rho_4 z^{-3}$$

This is equivalent to *ignoring all multiple reflections* within each layer and considering only a *single* reflection at each interface. Indeed, the term $\rho_2 z^{-1}$ represents the wave reflected at interface-2 and arriving back at interface-1 with a roundtrip delay of z^{-1}. Similarly, $\rho_3 z^{-2}$ represents the reflection at interface-3 and has a delay of z^{-2} because the wave must make a roundtrip of two layers to come back to interface-1, and $\rho_4 z^{-3}$ has three roundtrip delays because the wave must traverse three layers. □

The two MATLAB functions `frwrec` and `bkwrec` implement the forward and backward recursions (6.6.49) and (6.6.50), respectively. They have usage:

```
[A,B] = frwrec(r);          % forward recursion - from r to A,B
[r,A,B] = bkwrec(a,b);      % backward recursion - from a,b to r
```

The input r of `frwrec` represents the vector of the $M+1$ reflection coefficients and A, B are the $(M+1)\times(M+1)$ matrices whose columns are the polynomials $\mathbf{a}_i$ and $\mathbf{b}_i$ (padded with zeros at the end to make them of length $M+1$.) The inputs a, b of `bkwrec` are the final order-M polynomials $\mathbf{a}, \mathbf{b}$ and the outputs r, A, B have the same meaning as in `frwrec`. We note that the first row of B contains the reflection coefficients r.

The auxiliary functions `r2n` and `n2r` allow one to pass from the reflection coefficient vector r to the refractive index vector n, and conversely. They have usage:

```
n = r2n(r);              % reflection coefficients to refractive indices
r = n2r(n);              % refractive indices to reflection coefficients
```

As an illustration, the MATLAB code:

```
a = [1, -0.1, -0.064, -0.05];
b = [-0.1, -0.188, -0.35, 0.5];
[r,A,B] = bkwrec(a,b);
n = r2n(r);
r = n2r(n);
```

will generate the output of Example 6.6.1:

```
r =
   -0.1000   -0.2000   -0.4000    0.5000
A =
    1.0000    1.0000    1.0000    1.0000
   -0.1000   -0.1200   -0.2000         0
   -0.0640   -0.1000         0         0
   -0.0500         0         0         0
B =
   -0.1000   -0.2000   -0.4000    0.5000
   -0.1880   -0.3600    0.5000         0
   -0.3500    0.5000         0         0
    0.5000         0         0         0
n =
    1.0000    1.2222    1.8333    4.2778    1.4259
r =
   -0.1000   -0.2000   -0.4000    0.5000
```

Conversely, if the above r is the input to `frwrec`, the returned matrices A, B will be identical to the above. The function `r2n` solves Eq. (6.1.1) for n_i and always assumes that the refractive index of the leftmost medium is unity. Once the n_i are known, the function `multidiel` may be used to compute the reflection response at any set of frequencies or wavelengths.

6.7 Applications of Layered Structures

In addition to their application in dielectric thin-film and radome design, layered structures and the corresponding forward and backward layer recursions have a number of applications in other wave propagation problems, such as the design of broadband terminations of transmission lines, the analysis and synthesis of speech, geophysical signal processing for oil exploration, the probing of tissue by ultrasound, and the design of acoustic reflectors for noise control.

It is remarkable also that the same forward and backward recursions (6.6.49) and (6.6.50) are identical (up to reindexing) to the forward and backward Levinson recursions of *linear prediction* [833], with the layer structures being mathematically equivalent to the analysis and synthesis lattice filters. This connection is perhaps the reason behind the great success of linear prediction methods in speech and geophysical signal processing.

Moreover, the forward and backward layer recursions in their reflection forms, Eqs. (6.6.41) and (6.6.47), and impedance forms, Eqs. (6.6.42) and (6.6.48), are the essential mathematical tools for Schur's characterization of *lossless bounded real* functions in the z-plane and Richard's characterization of *positive real* functions in the s-plane and have been applied to network synthesis and to the development of transfer function stability tests, such as the Schur-Cohn test [853–867].

In all wave problems there are always *two* associated propagating field quantities playing the roles of the electric and magnetic fields. For forward-moving waves the ratio of the two field quantities is constant and equal to the *characteristic impedance* of the particular propagation medium for the particular type of wave.

For example, for transmission lines the two field quantities are the voltage and current along the line, for sound waves they are the pressure and particle volume velocity, and for seismic waves, the stress and particle displacement.

A transmission line connected to a multisegment impedance transformer and a load is shown in Fig. 6.7.1. The characteristic impedances of the main line and the segments are Z_a and $Z_1, \ldots, Z_M$, and the impedance of the load, Z_b. Here, the impedances $\{Z_a, Z_1, \ldots, Z_M, Z_b\}$, play the same role as $\{\eta_a, \eta_1, \ldots, \eta_M, \eta_b\}$ in the dielectric stack case.

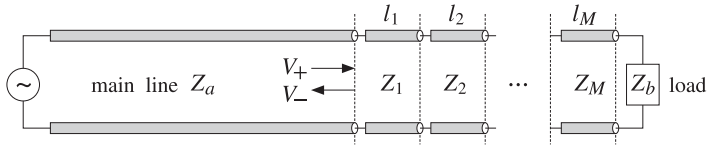

Fig. 6.7.1 Multisegment broadband termination of a transmission line.

The segment characteristic impedances Z_i and lengths l_i can be adjusted to obtain an overall reflection response that is reflectionless over a wideband of frequencies [822–832]. This design method is presented in Sec. 6.8.

In speech processing, the vocal tract is modeled as an acoustic tube of varying cross-sectional area. It can be approximated by the piece-wise constant area approximation shown in Fig. 6.7.2. Typically, ten segments will suffice.

The acoustic impedance of a sound wave varies inversely with the tube area, $Z = \rho c/A$, where ρ, c, and A are the air density, speed of sound, and tube area, respectively. Therefore, as the sound wave propagates from the glottis to the lips, it will suffer reflections every time it encounters an interface, that is, whenever it enters a tube segment of different diameter.

Multiple reflections will be set up within each segment and the tube will reverberate in a complicated manner depending on the number of segments and their diameters.

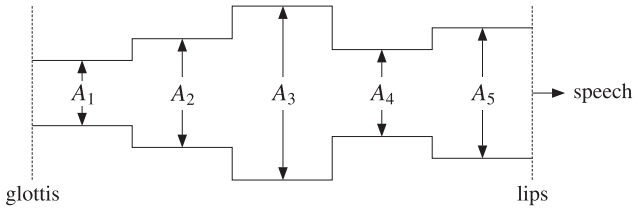

Fig. 6.7.2 Multisegment acoustic tube model of vocal tract.

By measuring the speech wave that eventually comes out of the lips (the transmission response,) it is possible to remove, or deconvolve, the reverberatory effects of the tube and, in the process, extract the tube parameters, such as the areas of the segments, or equivalently, the reflection coefficients at the interfaces.

During speech, the configuration of the vocal tract changes continuously, but it does so at mechanical speeds. For short periods of time (typically, of the order of 20–30 msec,) it may be considered to maintain a fixed configuration. From each such short segment of speech, a set of configuration parameters, such as reflection coefficients, is extracted. Conversely, the extracted parameters may be used to re-synthesize the speech segment.

Such linear prediction based acoustic tube models of speech production are routinely used in the analysis and synthesis of speech, speech recognition, speaker identification, and speech coding for efficient data transmission, such as in wireless phones.

The seismic problem in geophysical signal processing is somewhat different. Here, it is not the transmitted wave that is experimentally available, but rather the overall reflected wave. Fig. 6.7.3 shows the typical case.

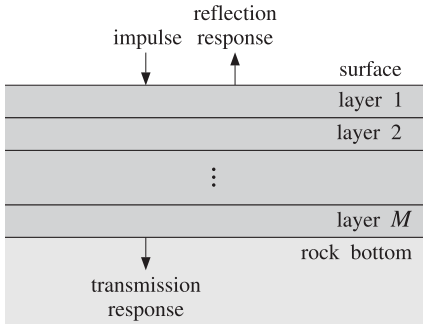

Fig. 6.7.3 Seismic probing of earth's multilayer structure.

An impulsive input to the earth, such as an explosion near the surface, will set up seismic elastic waves propagating downwards. As the various earth layers are encountered, reflections will take place. Eventually, each layer will be reverberating and an overall reflected wave will be measured at the surface. With the help of the backward

recursions, the parameters of the layered structure (reflection coefficients and impedances) are extracted and evaluated to determine the presence of a layer that contains an oil deposit.

The application of the backward recursions has been termed *dynamic predictive deconvolution* in the geophysical context [840–852]. An interesting historical account of the early development of this method by Robinson and its application to oil exploration and its connection to linear prediction is given in Ref. [846]. The connection to the conventional inverse scattering methods based on the *Gelfand-Levitan-Marchenko* approach is discussed in [847–852].

Fiber Bragg gratings (FBG), obtained by periodically modulating the refractive index of the core (or the cladding) of a finite portion of a fiber, behave very similarly to dielectric mirrors and exhibit high reflectance bands [788–808]. The periodic modulation is achieved by exposing that portion of the fiber to intense ultraviolet radiation whose intensity has the required periodicity. The periodicity shown in Fig. 6.7.4 can have arbitrary shape—not only alternating high/low refractive index layers as suggested by the figure. We discuss FBGs further in Sec. 12.4.

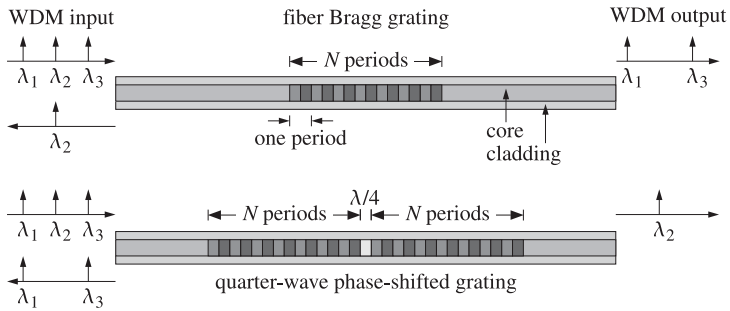

Fig. 6.7.4 Fiber Bragg gratings acting as bandstop or bandpass filters.

Quarter-wave phase-shifted fiber Bragg gratings act as narrow-band transmission filters and can be used as demultiplexing filters in WDM and dense WDM (DWDM) communications systems. Assuming as in Fig. 6.7.4 that the inputs to the FBGs consist of several multiplexed wavelengths, $\lambda_1, \lambda_2, \lambda_3, \ldots$, and that the FBGs are tuned to wavelength λ_2, then the ordinary FBG will act as an almost perfect reflector of λ_2. If its reflecting band is narrow, then the other wavelengths will transmit through. Similarly, the phase-shifted FBG will act as a narrow-band transmission filter allowing λ_2 through and reflecting the other wavelengths if they lie within its reflecting band.

A typical DWDM system may carry 40 wavelengths at 10 gigabits per second (Gbps) per wavelength, thus achieving a 400 Gbps bandwidth. In the near future, DWDM systems will be capable of carrying hundreds of wavelengths at 40 Gbps per wavelength, achieving terabit per second rates [808].

6.8 Chebyshev Design of Reflectionless Multilayers

In this section, we discuss the design of broadband reflectionless multilayer structures of the type shown in Fig. 6.6.1, or equivalently, broadband terminations of transmission lines as shown in Fig. 6.7.1, using Collin's method based on Chebyshev polynomials [822–832,657,676].

As depicted in Fig. 6.8.1, the desired specifications are: (a) the operating center frequency f_0 of the band, (b) the bandwidth Δf, and (c) the desired amount of attenuation A (in dB) within the desired band, measured with respect to the reflectance value at dc.

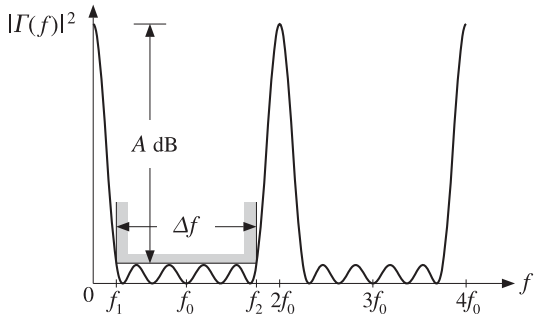

Fig. 6.8.1 Reflectance specifications for Chebyshev design.

Because the optical thickness of the layers is $\delta = \omega T_s/2 = (\pi/2)(f/f_0)$ and vanishes at dc, the reflection response at $f = 0$ should be set equal to its unmatched value, that is, to the value when there are no layers:

$$|\Gamma(0)|^2 = \rho_0^2 = \left(\frac{\eta_b - \eta_a}{\eta_a + \eta_b}\right)^2 = \left(\frac{n_a - n_b}{n_a + n_b}\right)^2 \tag{6.8.1}$$

Collin's design method [822] assumes $|\Gamma(f)|^2$ has the analytical form:

$$\boxed{|\Gamma(f)|^2 = \frac{e_1^2 T_M^2(x)}{1 + e_1^2 T_M^2(x)}} \qquad x = x_0 \cos\delta = x_0 \cos\left(\frac{\pi f}{2f_0}\right) \tag{6.8.2}$$

where $T_M(x) = \cos\big(M \operatorname{acos}(x)\big)$ is the Chebyshev polynomial (of the first kind) of order M. The parameters M, e_1, x_0 are fixed by imposing the desired specifications shown in Fig. 6.8.1.

Once these parameters are known, the order-M polynomials $A(z), B(z)$ are determined by spectral factorization, so that $|\Gamma(f)|^2 = |B(f)|^2/|A(f)|^2$. The backward layer recursions, then, allow the determination of the reflection coefficients at the layer interfaces, and the corresponding refractive indices. Setting $f = 0$, or $\delta = 0$, or $\cos\delta = 1$, or $x = x_0$, we obtain the design equation:

$$|\Gamma(0)|^2 = \frac{e_1^2 T_M^2(x_0)}{1 + e_1^2 T_M^2(x_0)} = \frac{e_0^2}{1 + e_0^2} = \rho_0^2 \tag{6.8.3}$$

where we defined $e_0 = e_1 T_M(x_0)$. Solving for e_0, we obtain:

$$\boxed{e_0^2 = \frac{\rho_0^2}{1 - \rho_0^2} = \frac{(n_a - n_b)^2}{4 n_a n_b}} \tag{6.8.4}$$

Chebyshev polynomials $T_M(x)$ are reviewed in more detail in Sec. 23.9 that discusses antenna array design using the Dolph-Chebyshev window. The two key properties of these polynomials are that they have *equiripple* behavior within the interval $-1 \le x \le 1$ and grow like x^M for $|x| > 1$; see for example, Fig. 23.9.1.

By adjusting the value of the scale parameter x_0, we can arrange the entire equiripple domain, $-1 \le x \le 1$, of $T_M(x)$ to be mapped onto the desired reflectionless band $[f_1, f_2]$, where f_1, f_2 are the left and right bandedge frequencies about f_0, as shown in Fig. 6.8.1. Thus, we demand the conditions:

$$x_0 \cos\left(\frac{\pi f_2}{2f_0}\right) = -1, \qquad x_0 \cos\left(\frac{\pi f_1}{2f_0}\right) = 1$$

These can be solved to give:

$$\begin{aligned} \frac{\pi f_2}{2f_0} &= \operatorname{acos}\left(-\frac{1}{x_0}\right) = \frac{\pi}{2} + \operatorname{asin}\left(\frac{1}{x_0}\right) \\ \frac{\pi f_1}{2f_0} &= \operatorname{acos}\left(\frac{1}{x_0}\right) = \frac{\pi}{2} - \operatorname{asin}\left(\frac{1}{x_0}\right) \end{aligned} \tag{6.8.5}$$

Subtracting, we obtain the bandwidth $\Delta f = f_2 - f_1$:

$$\frac{\pi}{2}\frac{\Delta f}{f_0} = 2 \operatorname{asin}\left(\frac{1}{x_0}\right) \tag{6.8.6}$$

We can now solve for the scale parameter x_0 in terms of the bandwidth:

$$\boxed{x_0 = \frac{1}{\sin\left(\frac{\pi}{4}\frac{\Delta f}{f_0}\right)}} \tag{6.8.7}$$

It is evident from Fig. 6.8.1 that the maximum value of the bandwidth that one can demand is $\Delta f_{\max} = 2f_0$. Going back to Eq. (6.8.5) and using (6.8.6), we see that f_1 and f_2 lie symmetrically about f_0, such that $f_1 = f_0 - \Delta f/2$ and $f_2 = f_0 + \Delta f/2$.

Next, we impose the attenuation condition. Because of the equiripple behavior over the Δf band, it is enough to impose the condition at the edges of the band, that is, we demand that when $f = f_1$, or $x = 1$, the reflectance is down by A dB as compared to its value at dc:

$$|\Gamma(f_1)|^2 = |\Gamma(0)|^2\, 10^{-A/10} \quad \Rightarrow \quad \frac{e_1^2 T_M^2(1)}{1 + e_1^2 T_M^2(1)} = \frac{e_0^2}{1 + e_0^2}\, 10^{-A/10}$$

But, $T_M(1) = 1$. Therefore, we obtain an equation for e_1^2:

$$\frac{e_1^2}{1 + e_1^2} = \frac{e_0^2}{1 + e_0^2}\, 10^{-A/10} \tag{6.8.8}$$

Noting that $e_0 = e_1 T_M(x_0)$, we solve Eq. (6.8.8) for the ratio $T_M(x_0) = e_0/e_1$:

$$T_M(x_0) = \cosh\big(M\,\text{acosh}(x_0)\big) = \sqrt{(1+e_0^2)\,10^{A/10} - e_0^2} \tag{6.8.9}$$

Alternatively, we can express A in terms of $T_M(x_0)$:

$$A = 10\log_{10}\left(\frac{T_M^2(x_0)+e_0^2}{1+e_0^2}\right) \tag{6.8.10}$$

where we used the definition $T_M(x_0) = \cosh\big(M\,\text{acosh}(x_0)\big)$ because $x_0 > 1$. Solving (6.8.9) for M in terms of A, we obtain:

$$\boxed{M = \text{ceil}(M_{\text{exact}})} \tag{6.8.11}$$

where

$$M_{\text{exact}} = \frac{\text{acosh}\left(\sqrt{(1+e_0^2)\,10^{A/10} - e_0^2}\right)}{\text{acosh}(x_0)} \tag{6.8.12}$$

Because M_{exact} is rounded up to the next integer, the attenuation will be somewhat larger than required. In summary, we calculate e_0, x_0, M from Eqs. (6.8.4), (6.8.7), and (6.8.11). Finally, e_1 is calculated from:

$$\boxed{e_1 = \frac{e_0}{T_M(x_0)} = \frac{e_0}{\cosh\big(M\,\text{acosh}(x_0)\big)}} \tag{6.8.13}$$

Next, we construct the polynomials $A(z)$ and $B(z)$. It follows from Eqs. (6.6.25) and (6.6.34) that the reflectance and transmittance are:

$$|\Gamma(f)|^2 = \frac{|B(f)|^2}{|A(f)|^2}, \quad |T(f)|^2 = 1 - |\Gamma(f)|^2 = \frac{\sigma^2}{|A(f)|^2},$$

Comparing these with Eq. (6.8.2), we obtain:

$$\begin{aligned} |A(f)|^2 &= \sigma^2\big[1 + e_1^2 T_M^2(x_0\cos\delta)\big] \\ |B(f)|^2 &= \sigma^2 e_1^2 T_M^2(x_0\cos\delta) \end{aligned} \tag{6.8.14}$$

The polynomial $A(z)$ is found by requiring that it be a minimum-phase polynomial, that is, with all its zeros inside the unit circle on the z-plane. To find this polynomial, we determine the $2M$ roots of the right-hand-side of $|A(f)|^2$ and keep only those M that lie inside the unit circle. We start with the equation for the roots:

$$\sigma^2\big[1 + e_1^2 T_M^2(x_0\cos\delta)\big] = 0 \quad \Rightarrow \quad T_M(x_0\cos\delta) = \pm\frac{j}{e_1}$$

Because $T_M(x_0\cos\delta) = \cos\big(M\,\text{acos}(x_0\cos\delta)\big)$, the desired M roots are given by:

$$x_0\cos\delta_m = \cos\left(\frac{\text{acos}(-\frac{j}{e_1}) + m\pi}{M}\right), \quad m = 0, 1, \ldots, M-1 \tag{6.8.15}$$

Indeed, these satisfy:

$$\cos\big(M\,\text{acos}(x_0\cos\delta_m)\big) = \cos\left(\text{acos}(-\frac{j}{e_1}) + m\pi\right) = -\frac{j}{e_1}\cos m\pi = \pm\frac{j}{e_1}$$

Solving Eq. (6.8.15) for δ_m, we find:

$$\boxed{\delta_m = \text{acos}\left[\frac{1}{x_0}\cos\left(\frac{\text{acos}(-\frac{j}{e_1}) + m\pi}{M}\right)\right]}, \quad m = 0, 1, \ldots, M-1 \tag{6.8.16}$$

Then, the M zeros of $A(z)$ are constructed by:

$$\boxed{z_m = e^{2j\delta_m}}, \quad m = 0, 1, \ldots, M-1 \tag{6.8.17}$$

These zeros lie inside the unit circle, $|z_m| < 1$. (Replacing $-j/e_1$ by $+j/e_1$ in Eq. (6.8.16) would generate M zeros that lie outside the unit circle; these are the zeros of $\tilde{A}(z)$.) Finally, the polynomial $A(z)$ is obtained by multiplying the root factors:

$$A(z) = \prod_{m=0}^{M-1}(1 - z_m z^{-1}) = 1 + a_1 z^{-1} + a_2 z^{-2} + \cdots + a_M z^{-M} \tag{6.8.18}$$

Once $A(z)$ is obtained, we may fix the scale factor σ^2 by requiring that the two sides of Eq. (6.8.14) match at $f = 0$. Noting that $A(f)$ at $f = 0$ is equal to the sum of the coefficients of $A(z)$ and that $e_1 T_M(x_0) = e_0$, we obtain the condition:

$$\left|\sum_{m=0}^{M-1} a_m\right|^2 = \sigma^2(1+e_0^2) \quad \Rightarrow \quad \sigma = \pm\frac{\left|\sum_{m=0}^{M-1} a_m\right|}{\sqrt{1+e_0^2}} \tag{6.8.19}$$

Either sign of σ leads to a solution, but its physical realizability (i.e., $n_1 \geq 1$) requires that we choose the negative sign if $n_a < n_b$, and the positive one if $n_a > n_b$. (The opposite choice of signs leads to the solution $n_i' = n_a^2/n_i$, $i = a, 1, \ldots, M, b$.)

The polynomial $B(z)$ can now be constructed by taking the square root of the second equation in (6.8.14). Again, the simplest procedure is to determine the roots of the right-hand side and multiply the root factors. The root equations are:

$$\sigma^2 e_1^2 T_M^2(x_0\cos\delta) = 0 \qquad \Rightarrow \qquad T_M(x_0\cos\delta) = 0$$

with M roots:

$$\delta_m = \text{acos}\left(\frac{1}{x_0}\cos\left(\frac{(m+0.5)\pi}{M}\right)\right), \quad m = 0, 1, \ldots, M-1 \tag{6.8.20}$$

The z-plane roots are $z_m = e^{2j\delta_m}$, $m = 0, 1, \ldots, M-1$. The polynomial $B(z)$ is now constructed up to a constant b_0 by the product:

$$B(z) = b_0\prod_{m=0}^{M-1}(1 - z_m z^{-1}) \tag{6.8.21}$$

As before, the factor b_0 is fixed by matching Eq. (6.8.14) at $f = 0$. Because δ_m is real, the zeros z_m will all have unit magnitude and $B(z)$ will be equal to its reverse polynomial, $B^R(z) = B(z)$.

Finally, the reflection coefficients at the interfaces and the refractive indices are obtained by sending $A(z)$ and $B(z)$ into the backward layer recursion.

The above design steps are implemented by the MATLAB functions `chebtr`, `chebtr2`, and `chebtr3` with usage:

```
[n,a,b]     = chebtr(na,nb,A,DF);          % Chebyshev multilayer design
[n,a,b,A]   = chebtr2(na,nb,M,DF);         % specify order and bandwidth
[n,a,b,DF] = chebtr3(na,nb,M,A);           % specify order and attenuation
```

The inputs are the refractive indices n_a, n_b of the left and right media, the desired attenuation in dB, and the fractional bandwidth $\Delta F = \Delta f/f_0$. The output is the refractive index vector $\mathbf{n} = [n_a, n_1, n_2, \ldots, n_M, n_b]$ and the reflection and transmission polynomials **b** and **a**. In `chebtr2` and `chebtr3`, the order M is given. To clarify the design steps, we give below the essential source code for `chebtr`:

```
e0 = sqrt((nb-na)^2/(4*nb*na));
x0 = 1/sin(DF*pi/4);
M = ceil(acosh(sqrt((e0^2+1)*10^(A/10) - e0^2))/acosh(x0));
e1 = e0/cosh(M*acosh(x0));

m=0:M-1;
delta = acos(cos((acos(-j/e1)+pi*m)/M)/x0);
z = exp(2*j*delta);                        % zeros of A(z)

a = real(poly(z));                         % coefficients of A(z)

sigma = sign(na-nb)*abs(sum(a))/sqrt(1+e0^2);   % scale factor σ

delta = acos(cos((m+0.5)*pi/M)/x0);
z = exp(2*j*delta);                        % zeros of B(z)

b = real(poly(z));                         % unscaled coefficients of B(z)
b0 = sigma * e0 / abs(sum(b));
b = b0 * b;                                % rescaled B(z)

r = bkwrec(a,b);                           % backward recursion
n = na * r2n(r);                           % refractive indices
```

Example 6.8.1: *Broadband antireflection coating.* Design a broadband antireflection coating on glass with $n_a = 1$, $n_b = 1.5$, $A = 20$ dB, and fractional bandwidth $\Delta F = \Delta f/f_0 = 1.5$. Then, design a coating with deeper and narrower bandwidth having parameters $A = 30$ dB and $\Delta F = \Delta f/f_0 = 1.0$.

Solution: The reflectances of the designed coatings are shown in Fig. 6.8.2. The two cases have $M = 8$ and $M = 5$, respectively, and refractive indices:

$$n = [1, 1.0309, 1.0682, 1.1213, 1.1879, 1.2627, 1.3378, 1.4042, 1.4550, 1.5]$$

$$n = [1, 1.0284, 1.1029, 1.2247, 1.3600, 1.4585, 1.5]$$

The specifications are better than satisfied because the method rounds up the exact value of M to the next integer. These exact values were $M_{\text{exact}} = 7.474$ and $M_{\text{exact}} = 4.728$, and were increased to $M = 8$ and $M = 5$.

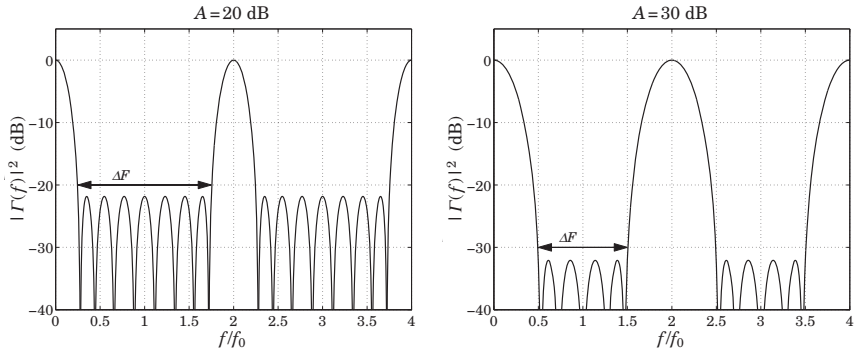

Fig. 6.8.2 Chebyshev designs. Reflectances are normalized to 0 dB at dc.

The desired bandedges shown on the graphs were computed from $f_1/f_0 = 1 - \Delta F/2$ and $f_1/f_0 = 1 + \Delta F/2$. The designed polynomial coefficients **a**, **b** were in the two cases:

$$\mathbf{a} = \begin{bmatrix} 1.0000 \\ 0.0046 \\ 0.0041 \\ 0.0034 \\ 0.0025 \\ 0.0017 \\ 0.0011 \\ 0.0005 \\ 0.0002 \end{bmatrix}, \quad \mathbf{b} = \begin{bmatrix} -0.0152 \\ -0.0178 \\ -0.0244 \\ -0.0290 \\ -0.0307 \\ -0.0290 \\ -0.0244 \\ -0.0178 \\ -0.0152 \end{bmatrix} \quad \text{and} \quad \mathbf{a} = \begin{bmatrix} 1.0000 \\ 0.0074 \\ 0.0051 \\ 0.0027 \\ 0.0010 \\ 0.0002 \end{bmatrix}, \quad \mathbf{b} = \begin{bmatrix} -0.0140 \\ -0.0350 \\ -0.0526 \\ -0.0526 \\ -0.0350 \\ -0.0140 \end{bmatrix}$$

The zeros of the polynomials **a** were in the two cases:

$$z = \begin{bmatrix} 0.3978\angle \pm 27.93^o \\ 0.3517\angle \pm 73.75^o \\ 0.3266\angle \pm 158.76^o \\ 0.3331\angle \pm 116.34^o \end{bmatrix} \quad \text{and} \quad z = \begin{bmatrix} 0.2112\angle \pm 45.15^o \\ 0.1564\angle 180^o \\ 0.1678\angle \pm 116.30^o \end{bmatrix}$$

They lie inside the unit circle by design. The typical MATLAB code used to generate these examples was:

```
na = 1; nb = 1.5; A = 20; DF = 1.5;

n = chebtr(na,nb,A,DF);
M = length(n) - 2;

f = linspace(0,4,1601);
L = 0.25 * ones(1,M);

G0 = (na-nb)^2 / (na+nb)^2;
G  = abs(multidiel(n,L,1./f)).^2;

plot(f, 10*log10(G/G0));
```

The reflectances were computed with the function `multidiel`. The optical thickness inputs to `multidiel` were all quarter-wavelength at f_0. □

We note, in this example, that the coefficients of the polynomial $B(z)$ are symmetric about their middle, that is, the polynomial is self-reversing $B^R(z) = B(z)$. One consequence of this property is that the vector of reflection coefficients is also symmetric about its middle, that is,

$$[\rho_1, \rho_2, \ldots, \rho_M, \rho_{M+1}] = [\rho_{M+1}, \rho_M, \ldots, \rho_2, \rho_1] \tag{6.8.22}$$

or, $\rho_i = \rho_{M+2-i}$, for $i = 1, 2, \ldots, M+1$. These conditions are equivalent to the following constraints among the resulting refractive indices:

$$\boxed{n_i n_{M+2-i} = n_a n_b \quad \Leftrightarrow \quad \rho_i = \rho_{M+2-i}}, \quad i = 1, 2, \ldots, M+1 \tag{6.8.23}$$

These can be verified easily in the above example. The proof of these conditions follows from the symmetry of $B(z)$. A simple argument is to use the single-reflection approximation discussed in Example 6.6.4, in which the polynomial $B(z)$ is to first-order in the ρ_is:

$$B(z) = \rho_1 + \rho_2 z^{-1} + \cdots + \rho_{M+1} z^{-M}$$

If the symmetry property $\rho_i = \rho_{M+2-i}$ were not true, then $B(z)$ could not satisfy the property $B^R(z) = B(z)$. A more exact argument that does not rely on this approximation can be given by considering the product of matrices (6.6.17).

In the design steps outlined above, we used MATLAB's built-in function `poly.m` to construct the numerator and denominator polynomials $B(z), A(z)$ from their zeros. These zeros are almost equally-spaced around the unit circle and get closer to each other with increasing order M. This causes `poly` to lose accuracy around order 50–60.

In the three `chebtr` functions (as well as in the Dolph-Chebyshev array functions of Chap. 23, we have used an improved version, `poly2.m`, with the same usage as `poly`, that maintains its accuracy up to order of about 3000.

Fig. 6.8.3 shows a typical pattern of zeros for Example 6.8.1 for normalized bandwidths of $\Delta F = 1.85$ and $\Delta F = 1.95$ and attenuation of $A = 30$ dB. The zeros of $B(z)$ lie on the unit circle, and those of $A(z)$, inside the circle. The function `poly2` groups the zeros in subgroups such that the zeros within each subgroup are not as closely spaced. For example, for the left graph of Fig. 6.8.3, `poly2` picks the zeros sequentially, whereas for the right graph, it picks every other zero, thus forming two subgroups, then `poly` is called on each subgroup, and the two resulting polynomials are convolved to get the overall polynomial.

Finally, we discuss the design of broadband terminations of transmission lines shown in Fig. 6.7.1. Because the media admittances are proportional to the refractive indices, $\eta_i^{-1} = n_i \eta_{\text{vac}}^{-1}$, we need only replace n_i by the line characteristic admittances:

$$[n_a, n_1, \ldots, n_M, n_b] \to [Y_a, Y_1, \ldots, Y_M, Y_b]$$

where Y_a, Y_b are the admittances of the main line and the load and Y_i, the admittances of the segments. Thus, the vector of admittances can be obtained by the MATLAB call:

```
Y = chebtr(Ya, Yb, A, DF);          % Chebyshev transmission line impedance transformer
```


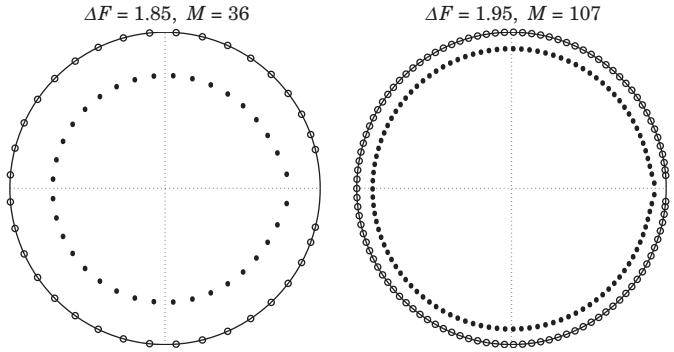

Fig. 6.8.3 Zero patterns of $B(z)$ (open circles) and $A(z)$ (filled circles), for $A = 30$ dB.

We also have the property (6.8.23), $Y_i Y_{M+2-i} = Y_a Y_b$, or, $Z_i Z_{M+2-i} = Z_a Z_b$, for $i = 1, 2, \ldots, M+1$, where $Y_i = 1/Z_i$. One can work directly with impedances—the following call would generate exactly the same solution, where $Z = [Z_a, Z_1, \ldots, Z_M, Z_b]$:

```
Z = chebtr(Za, Zb, A, DF);          % Chebyshev transmission line impedance transformer
```

In this design method, one does not have any control over the resulting refractive indices n_i or admittances Y_i. This can be problematic in the design of antireflection coatings because there do not necessarily exist materials with the designed n_is. However, one can replace or "simulate" any value of the refractive index of a layer by replacing the layer with an equivalent set of three layers of available indices and appropriate thicknesses [632–692].

This is not an issue in the case of transmission lines, especially microstrip lines, because one can design a line segment of a desired impedance by adjusting the geometry of the line, for example, by changing the diameters of a coaxial cable, the spacing of a parallel-wire, or the width of a microstrip line.

6.9 Problems

6.1 A uniform plane wave of frequency of 1.25 GHz is normally incident from free space onto a fiberglass dielectric slab ($\epsilon = 4\epsilon_0, \mu = \mu_0$) of thickness of 3 cm, as shown on the left figure below.

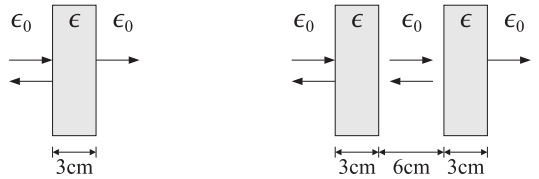

a. What is the free-space wavelength of this wave in cm? What is its wavelength inside the fiberglass?

b. What percentage of the incident power is reflected backwards?

c. Next, an identical slab is inserted to the right of the first slab at a distance of 6 cm, as shown on the right. What percentage of incident power is now reflected back?

6.2 Three identical dielectric slabs of thickness of 1 cm and dielectric constant $\epsilon = 4\epsilon_0$ are positioned as shown below. A uniform plane wave of frequency of 3.75 GHz is incident normally onto the leftmost slab.

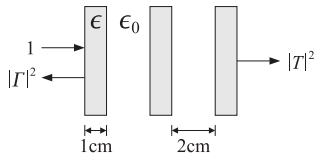

a. Determine the power reflection and transmission coefficients, $|\Gamma|^2$ and $|T|^2$, as percentages of the incident power.

b. Determine $|\Gamma|^2$ and $|T|^2$ if the three slabs and air gaps are replaced by a single slab of thickness of 7 cm.

6.3 Three identical fiberglass slabs of thickness of 3 cm and dielectric constant $\epsilon = 4\epsilon_0$ are positioned at separations $d_1 = d_2 = 6$ cm, as shown below. A wave of free-space wavelength of 24 cm is incident normally onto the left slab.

a. Determine the percentage of reflected power.

b. Repeat if the slabs are repositioned such that $d_1 = 12$ cm and $d_2 = 6$ cm.

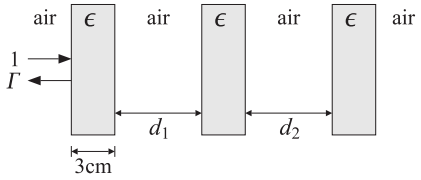

6.4 Four identical dielectric slabs of thickness of 1 cm and dielectric constant $\epsilon = 4\epsilon_0$ are positioned as shown below. A uniform plane wave of frequency of 3.75 GHz is incident normally onto the leftmost slab.

a. Determine the reflectance $|\Gamma|^2$ as a percentage.

b. Determine $|\Gamma|^2$ if slabs A and C are removed and replaced by air.

c. Determine $|\Gamma|^2$ if the air gap B between slabs A and C is filled with the same dielectric, so that ABC is a single slab.

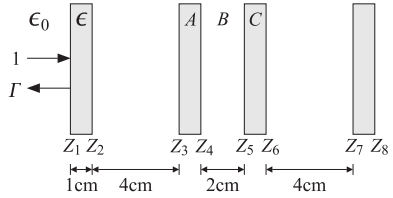

6.5 A 2.5 GHz wave is normally incident from air onto a dielectric slab of thickness of 2 cm and refractive index of 1.5, as shown below. The medium to the right of the slab has index 2.25.

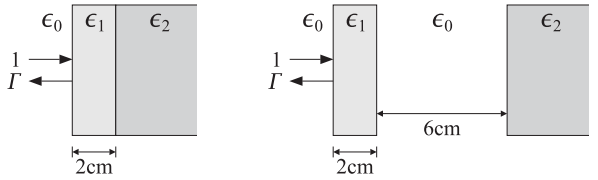

a. Derive an analytical expression of the reflectance $|\Gamma(f)|^2$ as a function of frequency and sketch it versus f over the interval $0 \le f \le 10$ GHz. What is the value of the reflectance at 2.5 GHz?

b. Next, the 2-cm slab is moved to the left by a distance of 6 cm, creating an air-gap between it and the rightmost dielectric. What is the value of the reflectance at 2.5 GHz?

6.6 Show that the antireflection coating design equations (6.2.2) can be written in the alternative forms:

$$\cos^2 k_2 l_2 = \frac{(n_2^2 - n_a n_b)\,(n_2^2 n_a - n_1^2 n_b)}{n_a\,(n_2^2 - n_b^2)\,(n_2^2 - n_1^2)}\,, \quad \sin^2 k_2 l_2 = \frac{n_2^2\,(n_b - n_a)\,(n_1^2 - n_a n_b)}{n_a\,(n_2^2 - n_b^2)\,(n_2^2 - n_1^2)}$$

Making the assumptions that $n_2 > n_1 > n_a$, $n_2 > n_b$, and $n_b > n_a$, show that for the design to have a solution, the following conditions must be satisfied:

$$n_1 > \sqrt{n_a n_b} \quad \text{and} \quad n_2 > n_1 \sqrt{\frac{n_b}{n_a}}$$

6.7 Show that the characteristic polynomial of any 2×2 matrix F is expressible in terms of the trace and the determinant of F as in Eq. (6.3.10), that is,

$$\det(F - \lambda I) = \lambda^2 - (\operatorname{tr} F)\lambda + \det F$$

Moreover, for a unimodular matrix show that the two eigenvalues are $\lambda_\pm = e^{\pm\alpha}$ where $\alpha = \operatorname{acosh}(a)$ and $a = \operatorname{tr} F/2$.

6.8 Show that the bandedge condition $a = -1$ for a dielectric mirror is equivalent to the condition of Eq. (6.3.16). Moreover, show that an alternative condition is:

$$\cos\delta_H \cos\delta_L - \frac{1}{2}\left(\frac{n_H}{n_L} + \frac{n_L}{n_H}\right)\sin\delta_H \sin\delta_L = -1$$

6.9 Stating with the approximate bandedge frequencies given in Eq. (6.3.19), show that the bandwidth and center frequency of a dielectric mirror are given by:

$$\Delta f = f_2 - f_1 = \frac{2 f_0 \operatorname{asin}(\rho)}{\pi(L_H + L_L)}\,, \quad f_c = \frac{f_1 + f_2}{2} = \frac{f_0}{2(L_H + L_L)}$$

where $L_H = n_H l_H/\lambda_0$, $L_L = n_L l_L/\lambda_0$, and λ_0 is a normalization wavelength, and f_0 the corresponding frequency $f_0 = c_0/\lambda_0$.

6.10 *Computer Experiment—Antireflection Coatings.* Compute and plot over the 400–700 nm visible band the reflectance of the following antireflection coatings on glass, defined by the refractive indices and normalized optical thicknesses:

a. $n = [1, 1.38, 1.5]$, $L = [0.25]$
b. $n = [1, 1.38, 1.63, 1.5]$, $L = [0.25, 0.50]$
c. $n = [1, 1.38, 2.2, 1.63, 1.5]$, $L = [0.25, 0.50, 0.25]$
d. $n = [1, 1.38, 2.08, 1.38, 2.08, 1.5]$, $L = [0.25, 0.527, 0.0828, 0.0563]$

The normalization wavelength is $\lambda_0 = 550$ nm. Evaluate and compare the coatings in terms of bandwidth. Cases (a-c) are discussed in Sec. 6.2 and case (d) is from [639].

6.11 *Computer Experiment—Dielectric Sunglasses.* A thin-film multilayer design of dielectric sunglasses was carried out in Ref. [1845] using 29 layers of alternating TiO_2 ($n_H = 2.35$) and SiO_2 ($n_L = 1.45$) coating materials. The design may be found on the web page: `www.sspectra.com/designs/sunglasses.html`.

The design specifications for the thin-film structure were that the transmittance be: (a) less than one percent for wavelengths 400–500 nm, (b) between 15–25 percent for 510–790 nm, and (c) less than one percent for 800–900 nm.

Starting with the high-index layer closest to the air side and ending with the high-index layer closest to the glass substrate, the designed lengths of the 29 layers were in nm (read across):

21.12	32.41	73.89	123.90	110.55	129.47
63.17	189.07	68.53	113.66	62.56	59.58
27.17	90.29	44.78	73.58	50.14	94.82
60.40	172.27	57.75	69.00	28.13	93.12
106.07	111.15	32.68	32.82	69.95	

Form the optical lengths $n_i l_i$ and normalize them $L_i = n_i l_i / \lambda_0$, such that the maximum optical length is a quarter wavelength at λ_0. What is the value of λ_0 in nm? Assuming the glass substrate has index $n = 1.5$, compute and plot the reflectance and transmittance over the band 400–900 nm.

6.12 *Computer Experiment—Dielectric Mirror.* Reproduce all the results and graphs of Example 6.3.2. In addition, carry out the computations for the cases of $N = 16, 32$ bilayers.

In all cases, calculate the minimum and maximum reflectance within the high-reflectance band. For one value of N, calculate the reflectance using the closed-form expression (6.3.33) and verify that it is the same as that produced by `multidiel`.

6.13 *Computer Experiment—Dielectric Mirror.* Reproduce all the results and graphs of Example 6.3.3. Repeat the computations and plots when the number of bilayers is $N = 8, 16$. Repeat for $N = 4, 8, 16$ assuming the layers are quarter-wavelength layers at 12.5 μm. In all cases, calculate the minimum and maximum reflectance within the high-reflectance band.

6.14 *Computer Experiment—Shortpass and Longpass Filters.* Reproduce all the results and graphs of Example 6.3.5. Redo the experiments by shifting the short-pass wavelength to $\lambda_0 = 750$ nm in the first case, and the long-pass wavelength to $\lambda_0 = 350$ nm in the second case. Plot the reflectances over the extended band of 200–1000 nm.

6.15 *Computer Experiment—Wide Infrared Bandpass Filter.* A 47-layer infrared bandpass filter with wide transmittance bandwidth was designed in Ref. [1845]. The design may be found on the web page `www.sspectra.com/designs/irbp.html`.

The alternating low- and high-index layers were ZnS and Ge with indices 2.2 and 4.2. The substrate was Ge with index 4. The design specifications were that the transmittance be: (a)

less than 0.1% for wavelengths 2–3 μm, (b) greater than 99% for 3.3–5 μm, and (c) less than 0.1% for 5.5–7 μm.

Starting with a low-index layer near the air side and ending with a low-index layer at the substrate, the layer lengths were in nm (read across):

528.64	178.96	250.12	123.17	294.15	156.86	265.60	134.34
266.04	147.63	289.60	133.04	256.22	165.16	307.19	125.25
254.28	150.14	168.55	68.54	232.65	125.48	238.01	138.25
268.21	98.28	133.58	125.31	224.72	40.79	564.95	398.52
710.47	360.01	724.86	353.08	718.52	358.23	709.26	370.42
705.03	382.28	720.06	412.85	761.47	48.60	97.33	

Form the optical lengths $n_i l_i$ and normalize them $L_i = n_i l_i / \lambda_0$, such that the maximum optical length is a quarter wavelength at λ_0. What is the value of λ_0 in μm? Compute and plot the reflectance and transmittance over the band 2–7 μm.

6.16 The figure below shows three multilayer structures. The first, denoted by $(LH)^3$, consists of three identical bilayers, each bilayer consisting of a low-index and a high-index quarter-wave layer, with indices $n_L = 1.38$ and $n_H = 3.45$. The second multilayer, denoted by $(HL)^3$, is the same as the first one, but with the order of the layers reversed. The third one, denoted by $(LH)^3(LL)(HL)^3$ consists of the first two side-by-side and separated by two low-index quarter-wave layers LL.

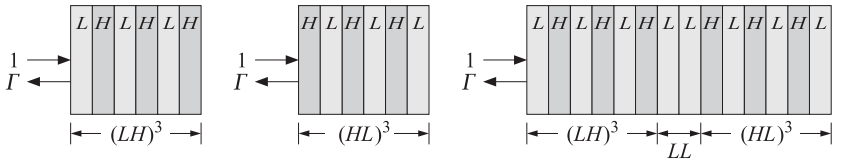

In all three cases, determine the overall reflection response Γ, as well as the percentage of reflected power, at the design frequency at which the individual layers are quarter-wave.

6.17 A radome protecting a microwave transmitter consists of a three-slab structure as shown below. The medium to the left and right of the structure is air. At the carrier frequency of the transmitter, the structure is required to be reflectionless, that is, $\Gamma = 0$.

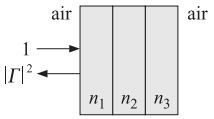

a. Assuming that all three slabs are quarter-wavelength at the design frequency, what should be the relationship among the three refractive indices n_1, n_2, n_3 in order to achieve a reflectionless structure?

b. What should be the relationship among the refractive indices n_1, n_2, n_3 if the middle slab (i.e., n_2) is half-wavelength but the other two are still quarter-wavelength slabs?

c. For case (a), suppose that the medium to the right has a slightly different refractive index from that of air, say, $n_b = 1 + \epsilon$. Calculate the small resulting reflection response Γ to first order in ϵ.

6.18 In order to obtain a reflectionless interface between media n_a and n_b, two dielectric slabs of equal optical lengths L and refractive indices n_b, n_a are positioned as shown below. (The same technique can be used to connect two transmission lines of impedances Z_a and Z_b.)

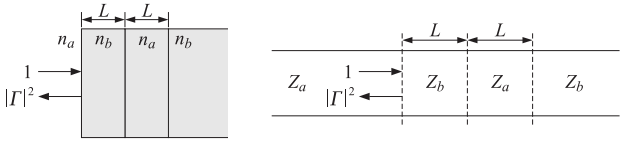

A plane wave of frequency f is incident normally from medium n_a. Let f_0 be the frequency at which the structure must be reflectionless. Let L be the common optical length normalized to the free-space wavelength $\lambda_0 = c_0/f_0$, that is, $L = n_a l_a/\lambda_0 = n_b l_b/\lambda_0$.

a. Show that the reflection response into medium n_a is given by:

$$\Gamma = \rho \frac{1 - (1+\rho^2)e^{-2j\delta} + e^{-4j\delta}}{1 - 2\rho^2 e^{-2j\delta} + \rho^2 e^{-4j\delta}}, \quad \rho = \frac{n_a - n_b}{n_a + n_b}, \quad \delta = 2\pi L \frac{f}{f_0}$$

b. Show that the interface will be reflectionless at frequency f_0 provided the optical lengths are chosen according to:

$$L = \frac{1}{4\pi} \arccos\left(\frac{1+\rho^2}{2}\right)$$

This is known as a *twelfth-wave* transformer because for $\rho = 0$, it gives $L = 1/12$.

6.19 A lossless dielectric slab of refractive index n_1 and thickness l_1 is positioned at a distance l_2 from a semi-infinite dielectric of refractive index n_2, as shown below.

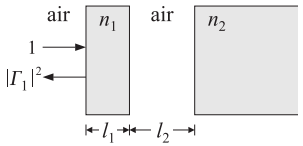

A uniform plane wave of free-space wavelength λ_0 is incident normally on the slab from the left. Assuming that the slab n_1 is a quarter-wavelength slab, determine the length l_2 (in units of λ_0) and the relationship between n_1 and n_2 in order that there be no reflected wave into the leftmost medium (i.e., $\Gamma_1 = 0$).

6.20 In order to provide structural strength and thermal insulation, a radome is constructed using two identical dielectric slabs of length d and refractive index n, separated by an air-gap of length d_2, as shown below.

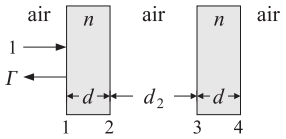

Recall that a reflectionless single-layer radome requires that the dielectric layer have half-wavelength thickness.

However, show that for the above dual-slab arrangement, either half- or quarter-wavelength dielectric slabs may be used, provided that the middle air-gap is chosen to be a half-wavelength layer, i.e., $d_2 = \lambda_0/2$, at the operating wavelength λ_0. [*Hint:* Work with wave impedances at the operating wavelength.]

6.21 *Computer Experiment—Dielectric Mirror Bands.* Consider the trace function given by Eq. (6.3.13) of the text, that is,

$$a = \frac{\cos(\delta_H + \delta_L) - \rho^2 \cos(\delta_H - \delta_L)}{1 - \rho^2}$$

The purpose of this problem is to study a as a function of frequency, which enters through:

$$\delta_i = 2\pi \left(\frac{f}{f_0}\right) L_i, \quad L_i = \frac{n_i l_i}{\lambda_0}, \quad i = H, L$$

and to identify the frequency bands where a switches from $|a| \le 1$ to $|a| \ge 1$, that is, when the dielectric mirror structure switches from transmitting to reflecting.

a. For the parameters given in Example 6.3.2 of the text, make a plot of a versus f over the range $0 \le f \le 4f_0$, using f/f_0 as your x-axis. Place on the graph the left and right bandedge frequencies f_1, f_2 of the reflecting bands centered at f_0 and odd multiples thereof.

b. Repeat for the parameters $n_a = 1$, $n_H = 4.6$, $n_L = 1.6$, $L_H = 0.3$, $L_L = 0.2$. These parameters are close to those of Example 6.3.2. You may use the function `omniband` to calculate the left and right bandedge frequencies around f_0.

In plotting a versus f/f_0, you will notice that a can become greater than $+1$ near $f = 2f_0$. Determine the left and right bandedge frequencies around $2f_0$ and check to see whether they define another reflecting band around $2f_0$.